神経細胞における低分子量GTP結合蛋白質Rhoを介した機能及びその作用機序に関する研究

２０００

加藤　裕教

A Study for Functions and Signal Transductions of Small GTPase Rho in Neuronal Cells

2000

Hironori Katoh

A Study for Functions and Signal Transductions of Small GTPase Rho in Neuronal Cells

2000

Hironori Katoh

CONTENTS

INTRODUCTION

The function of the nervous system depends on the highly specific pattern of connections formed between neurons during development. The specificity of these connections requires neurite extension toward the correct targets guided by the growth cone, and refinement and remodeling of the initial pattern of connections, referred to as synaptic plasticity, that are dependent on patterns of synaptic activity (1). The growth cone receives several kinds of environmental signals, such as diffusible chemoattractants and chemorepellants, extracellular matrix components, and cell adhesion molecules (2), and then the growth cone interprets these signals to generate a change in its shape and motility, that results in the advance, turning, or collapse of the growth cone.

The Rho family of small GTPases, including Rac, Cdc42, and Rho, has been implicated in the reorganization of the actin cytoskeleton and subsequent morphological changes in various cell types (3, 4). Like other GTPases of the Ras superfamily, they serve as molecular swithes by cycling between an inactive GDP-bound state and an active GTP-bound state. Activation of the Rho family proteins requires GDP-GTP exchange catalysed by various guanine-nucleotide exchange factors (GEFs), and their activation is also regulated by GTPase-activating proteins (GAPs) which stimulate their intrinsic GTPase activities. In addition, guanine-nucleotide dissociation inhibitors (GDIs) inhibit the exchange of GDP for GTP and might also serve to regulate their association with membranes (Fig. 0-1). Recent studies have shown that the Rho family proteins play critical roles in the regulation of the cytoskeleton required for neurite extension and retraction. Studies on neuronal cell lines have shown that Rac and Cdc42 are involved in the formation of lamellipodia and filopodia of the growth cone,

respectively, and they are required for the outgrowth of neurites. On the other hand, Rho is required for the collapse of the growth cone and the retraction of neurites (5-7, Fig. 0-2). The functions of these GTPases have been also examined *in vivo*, and defects in the regulation of these GTPase activities have been demonstrated to affect the development of the nervous system (8-10).

PC12 cells are derived from rat pheochromocytomas and serve as a useful model system for the study of neuronal differentiation. When PC12 cells are exposed to nerve growth factor (NGF) for several days, they acquire many features of sympathetic neurons, such as outgrowth of neurites (11). Previous studies have found that the activation of a certain heterotrimeric GTP-binding protein (G-protein)-coupled receptor, such as lysophosphatidic acid (LPA) receptor, caused the rapid collapse of growth cones and retraction of extended neurites in NGF-differentiated PC12 cells (12-14). *Clostridium botulinum* C3 exoenzyme, which specifically ADP-ribosylates Rho and suppresses the actions of Rho (15, 16), inhibits the receptor-mediated growth cone collapse and neurite retraction (17, 18), indicating that Rho is required for these morphological changes. However, the intracellular mechanisms involved in Rho-mediated morphological changes in neuronal cells have not yet been elucidated.

In this study, the auther has investigated the signal transduction pathways upstream and downstream of Rho to induce growth cone collapse and neurite retraction in NGF-differentiated PC12 cells. The results obtained are described in the following, divided into three chapters.

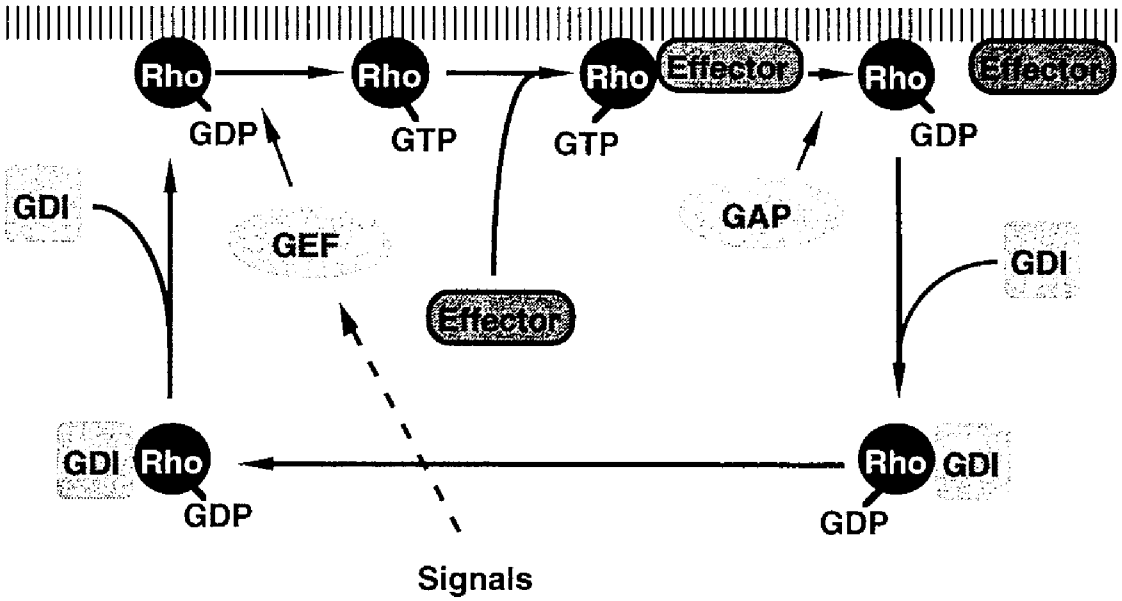

Fig. 0-1. GDP-GTP cycle of Rho.

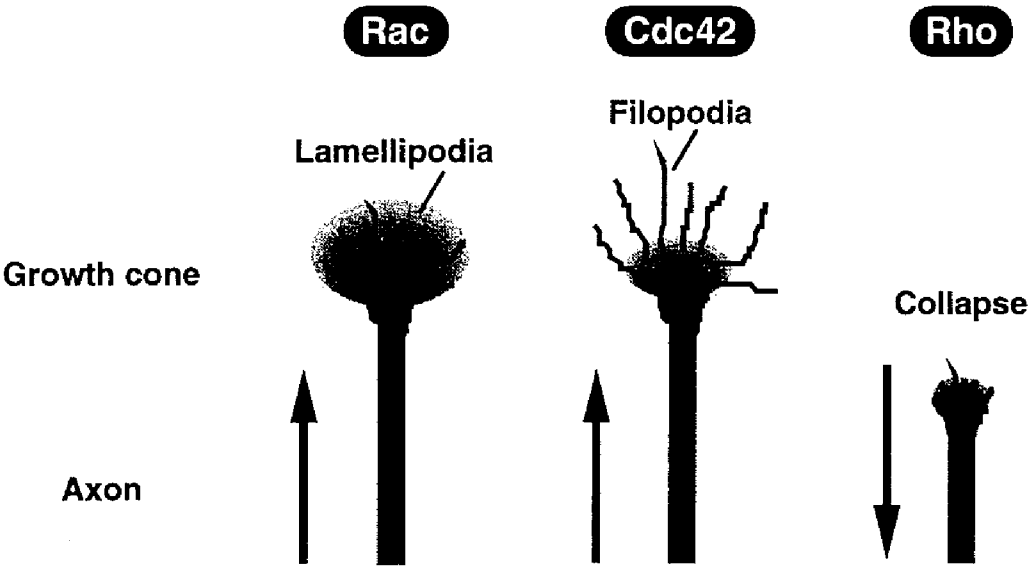

Fig. 0-2. Roles of Rho family small G proteins in navigation of the growth cone.

Abbreviations used in the text

GEF, guanine nucleotide exchange factor

GAP, GTPase-activating protein

GDI, guanine nucleotide dissociation inhibitor

NGF, nerve growth factor

G protein, GTP-binding protein

LPA, lysophosphatidic acid

PH, pleckstrin homology

GST, glutathione-S-transferase

MLC, myosin light chain

PT, pertussis toxin

PCR, polymerase chain reaction

PKC, protein kinase C

TPA, 12-*O*-tetradecanoylphorbol-13-acetate

PLC, phospholipase C

PG, prostaglandin

PKA, protein kinase A

Bt_2cAMP, dibutyryl cAMP

DMEM, Dulbecco's modified Eagle's medium

1. p160 RhoA-binding Kinase ROKα Induces Neurite Retraction

Summary

It is well known that activation of Rho by extracellular simuli, such as LPA, causes neurite retraction through small GTPase Rho in NGF-differentiated PC12 cells. However, a potential downstream effector of Rho to induce neurite retraction was not identified. Here I examined the effect of p160 RhoA-binding kinase ROKα, a target for RhoA recently identified, on the morphology of NGF-differentiated PC12 cells. Microinjection of the catalytic domain of ROKα rapidly induced neurite retraction similar to that induced by microinjection of a constitutively active RhoA, $RhoA^{V14}$, while microinjection of the kinase-deficient catalytic domain of ROKα did not induce neurite retraction. This morphological change was occurred even though C3 exoenzyme, which was known to inactivate Rho, had been preinjected. On the other hand, microinjection of the Rho-binding domain or the pleckstrin-homology domain of ROKα inhibited the prostaglandin EP3 receptor-induced neurite retraction. These results demonstrate that ROKα induces neurite retraction acting downstream of Rho in neuronal cells.

Introduction

When cells are activated by extracellular stimuli, inactive GDP-bound form of Rho is converted to active GTP-bound form of Rho, and once activated, Rho probably interacts with its specific targets, leading to a variety of biological functions (Fig. 0-1). Recently, several target proteins that interact only with GTP-bound form of Rho have been identified, including p128 protein kinase N (19, 20), p160 RhoA-binding kinase ROKα (21) also known as its bovine counterpart Rho-kinase (22) or its mouse counterpart ROCK-II (23), rhophilin (19), rhotekin (24), and p140mDia (25). Among them, ROKα has been reported to be involved in several functions of Rho: the regulation of myosin phosphorylation (26, 27), the formation of stress fibers and focal adhesions (28, 29), and the regulation of cytokinesis (30).

In NGF-differentiated PC12 cells, activation of Rho by several extracellular stimuli causes collapse of growth cones and retraction of extended neurites (18, 31). These effects appear to be induced by the contractility of the actin-based cytoskeleton (17, 32). However, a downstream effector of Rho to induce neurite retraction has not yet been identified. In the present study, I have examined the putative role of ROKα in the receptor-mediated neurite retraction in the NGF-differentiated PC12 cells. I demonstrate that ROKα is involved in the receptor-mediated neurite retraction acting downstream of Rho and that the activation of ROKα is sufficient for inducing neurite retraction.

Results

Neurite Retraction Induced by RhoA^{V14}

I obtained the evidence that M&B28767, an EP3 receptor agonist, induced neurite retraction in the EP3 receptor-expressing PC12 cells, and that this morphological change was completely inhibited when the cells were microinjected with C3 exoenzyme, which ADP-ribosylates and inactivates Rho (15, 16), indicating that the activation of Rho was required for the EP3 receptor-induced neurite retraction (31, also see Chapter 3). To determine whether activation of Rho is sufficient for inducing neurite retraction in the PC12 cells, I microinjected a constitutively activated recombinant RhoA, RhoA^{V14}, into the NGF-differentiated PC12 cells and examined its effect. Microinjection of RhoA^{V14} into the cytoplasm caused retraction of the neurites within 30 min (Fig. 1-1, *C* and *D*). More than 70% of the injected cells retracted their neurites (Fig. 1-5). This morphological change was similar to that stimulated by M&B28767 (Fig. 1-1, *A* and *B*). The neurite-retracted cells by microinjection of RhoA^{V14} was not stainined with trypan blue (data not shown), indicating that they did not undergo cell death. On the other hand, RhoA^{V14} containing a T37A substitution in the effector region, RhoA^{V14A37}, had no effect on the differentiated cells after microinjection (Fig. 1-1, *E* and *F*, and Fig. 1-5), suggesting that this mutation blocked the interaction of RhoA with its target to induce neurite retraction. This result also indicated that there were not any nonspecific effects due to the microinjection itself.

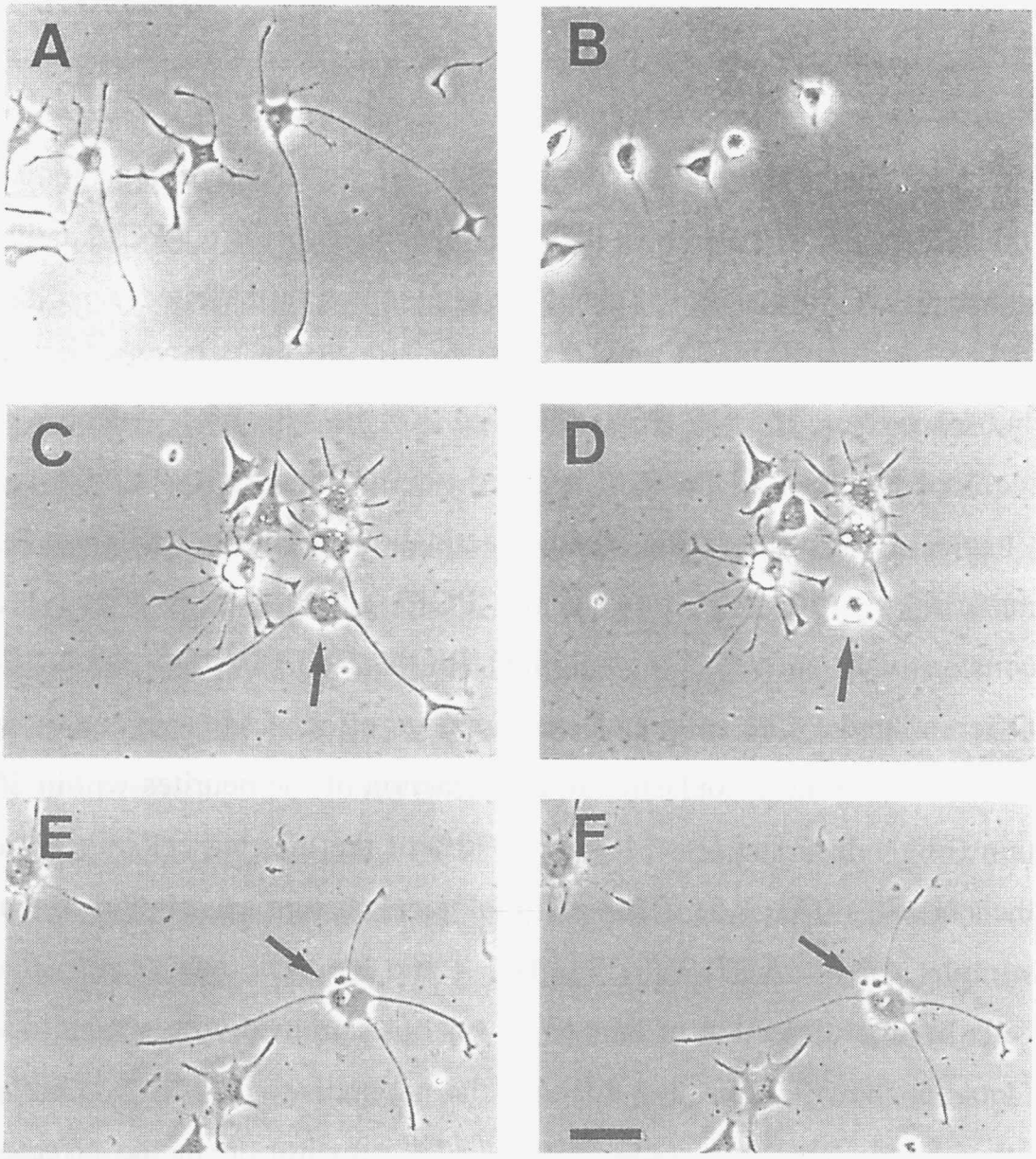

Figure 1-1. Neurite retraction induced by M&B28767 or microinjection of RhoA^{V14}. *A* and *B*, M&B28767-induced neurite retraction. The cells were differentiated with NGF for 3 days and photographed before (*A*) and 30 min after (*B*) addition of 1 μM M&B28767. *C* and *D*, microinjection of RhoA^{V14}. The cells were differentiated with NGF for 3 days and photographed before (*C*) and 30 min after (*D*) microinjection of 1 mg/ml of RhoA^{V14}. *E* and *F*, microinjection of RhoA^{V14A37}. The cells were differentiated with NGF for 3 days and photographed before (*C*) and 30 min after (*D*) microinjection of 1 mg/ml of RhoA^{V14A37}. The *arrows* indicate injected cells. The results shown are representative of three independent experiments. The *bar* represents 50 μm.

Neurite Retraction Induced by ROKα

Previous studies have suggested that the generation of actin-based contractile forces was required for neurite retraction (17, 32). Among several targets of Rho, ROKα appears to participate in Rho-dependent contractile events, such as the formation of stress fibers (28, 29) and the regulation of cytokinesis (30). By Northern blot analysis, ROKα was expressed in the NGF-differentiated PC12 cells (data not shown). Therefore, I examined whether ROKα was involved in the Rho-mediated neurite retraction in the NGF-differentiated PC12 cells. ROKα contains the catalytic domain in its amino-terminus, the coiled-coil domain, the Rho-binding domain, and the pleckstrin homology (PH) domain in its carboxy-terminus (Fig. 1-2). It was recently shown that the truncation mutant of ROKα containing the catalytic domain displayed constitutive kinase activity without addition of an active form

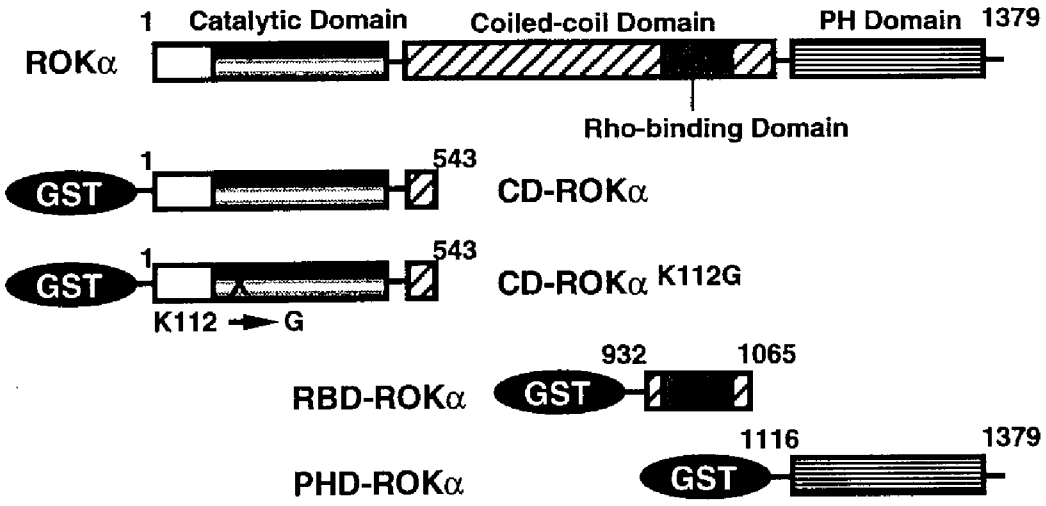

Fig. 1-2. Structure of ROKα.

of Rho, while the Rho-binding domain and the PH domain of ROKα served as dominant negative forms of the kinase (28, 29). Based on these characters, we generated recombinant proteins containing these domains as fusion proteins with gulutathione S-transferase (GST): the catalytic domain of ROKα (CD-ROKα, amino acids 1-543), the kinase-deficient mutant of CD-ROKα (CD-ROKα^{K112G}), the Rho-binding domain of ROKα (RBD-ROKα, amino acids 932-1065), and the PH domain of ROKα (PHD-ROKα, amino acids 1116-1379) (Fig. 1-2). To confirm that CD-ROKα really displayed constitutive kinase activity, I examined its kinase activity using myosin light chain (MLC) as a substrate. As shown in Fig. 1-3, CD-ROKα phosphorylated MLC, while CD-ROKα^{K112G} or RBD-ROKα did not, indicating that CD-ROKα is constitutively active. Then I microinjected these recombinant proteins into the NGF-differentiated cells and analyzed their morphologies.

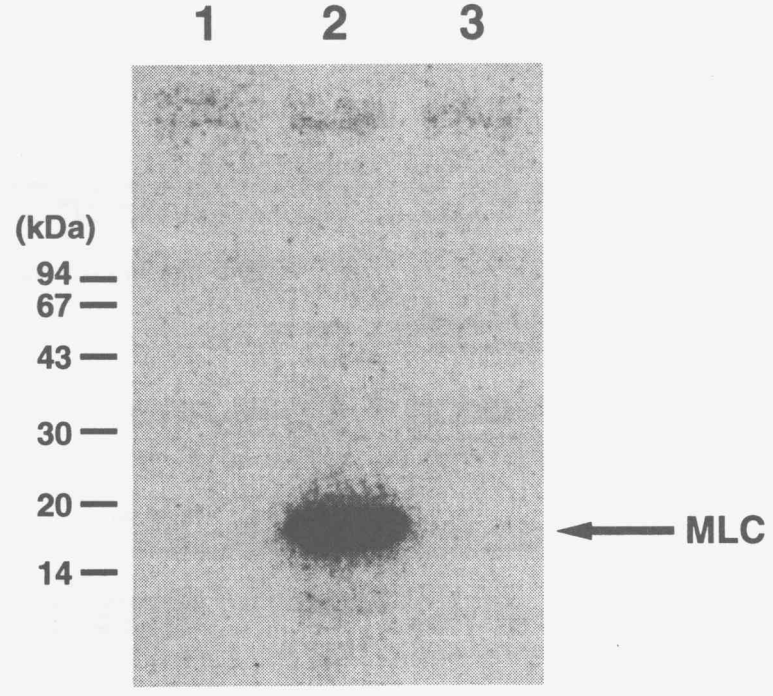

Figure 1-3. Phosphorylation of MLC by ROKα. Isolated MLC (4 μg) was incubated with 10 ng GST-RBD (lane 1), GST-CD-ROKα (lane 2), or GST-CD-ROKα^{K112G} (lane 3) for 10 min at 30°C. Phosphorylated MLC was resolved by SDS-PAGE and visualized by an image analyzer. The results shown are representative of three independent experiments.

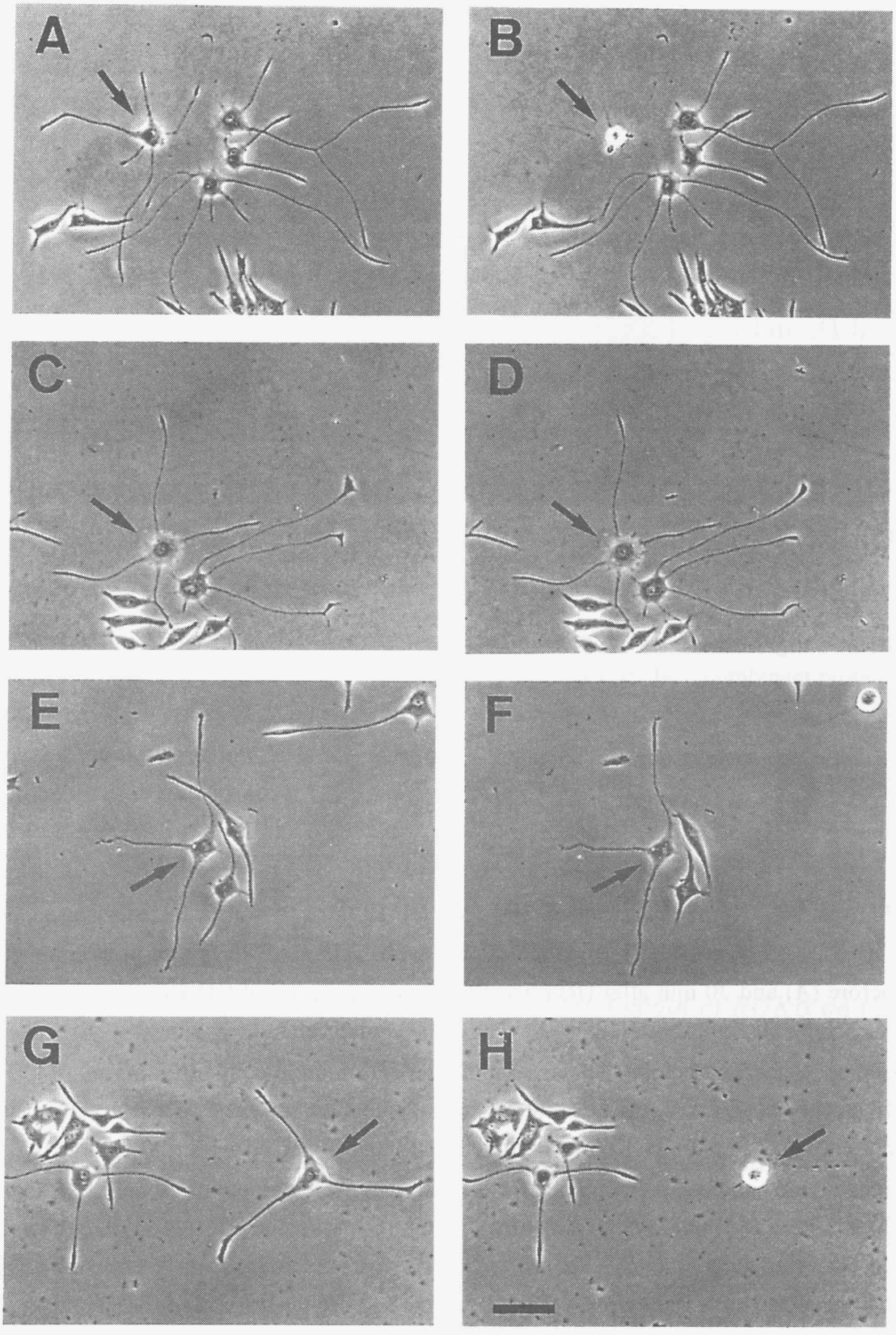
A
B
C
D
E
F
G
H

After the cells had been microinjected with CD-ROKα, they rapidly retracted their neurites within 30 min (Fig. 1-4, *A* and *B*, and Fig. 5). This morphological change was similar to that induced by microinjection of $RhoA^{V14}$. The neurite-retracted cells by microinjection of CD-ROKα was not stainined with trypan blue (data not shown), indicating that they did not undergo cell death. On the other hand, microinjection of CD-$ROK\alpha^{K112G}$ had no effect (Fig. 1-4, *C* and *D*, and Fig. 1-5), indicating that the kinase activity of CD-ROKα was required for inducing neurite retraction. When the cells were microinjected with C3 exoenzyme, the M&B28767-induced neurite retraction was completely suppressed (Fig. 1-4, *E* and *F*). However, the CD-ROKα-induced neurite retraction was not inhibited after the cells had been microinjected with C3 exoenzyme (Fig. 1-4, *G* and *H*), indicating that CD-ROKα acted downstream of Rho.

Figure 1-4. Neurite retraction induced by ROKα. *A* and *B*, microinjection of CD-ROKα. The cells were differentiated with NGF for 3 days and photographed before (*A*) and 30 min after (*B*) microinjection of 2 mg/ml of CD-ROKα. *C* and *D*, microinjection of CD-$ROK\alpha^{K112G}$. The cells were differentiated with NGF for 3 days and photographed before (*C*) and 30 min after (*D*) microinjection of 2 mg/ml of CD-$ROK\alpha^{K112G}$. *E* and *F*, the effect of C3 exoenzyme on the M&B28767-induced neurite retraction. After the NGF-differentiated cells microinjected with 100 μg/ml of C3 exoenzyme had been preincubated for 30 min, they were photographed before (*E*) and 30 min after (*F*) addition of 1 μM M&B28767. *G* and *H*, the effect of C3 exoenzyme on the CD-ROKα-induced neurite retraction. After the NGF-differentiated cells microinjected with 100 μg/ml of C3 exoenzyme had been preincubated for 30 min, they were photographed before (*G*) and 30 min after (*H*) microinjection of 2 mg/ml of CD-ROKα. The *arrows* indicate injected cells. The results shown are representative of three independent experiments. The *bar* represents 50 μm.

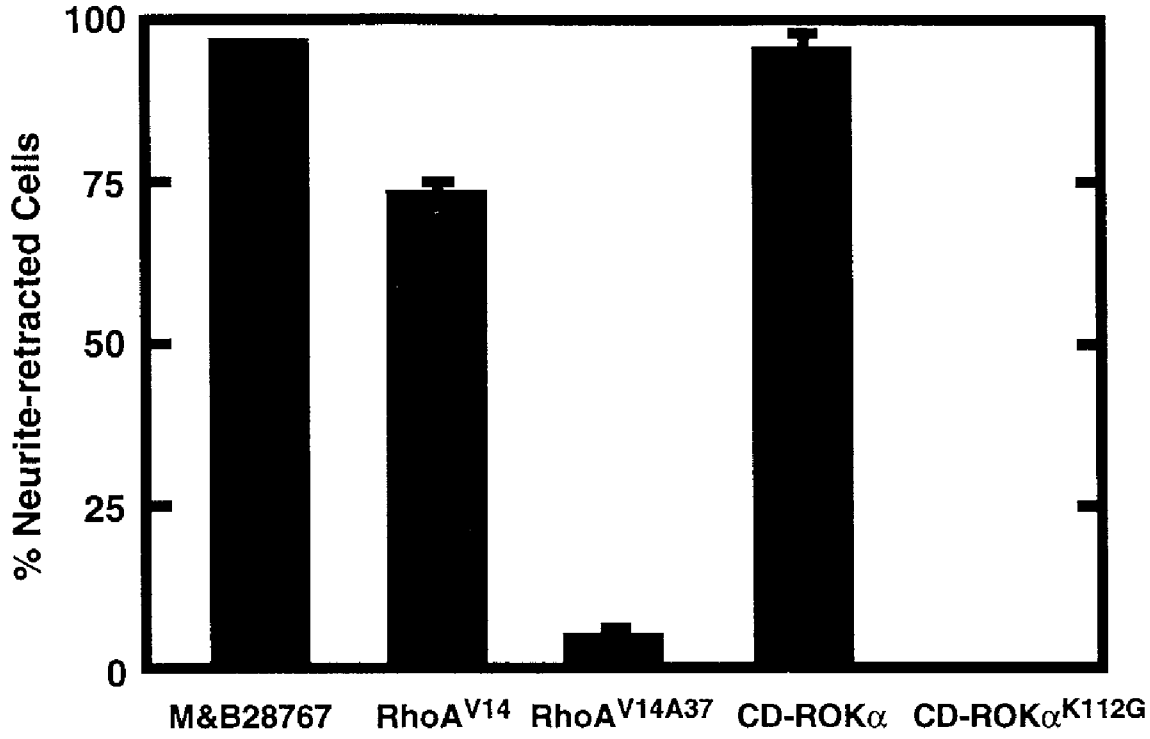

Figure 1-5. Quantification of effects of M&B28767, RhoA, and ROKα on neurite retraction. After the cells had been differentiated with NGF for 3 days, they were exposed to 1 μM M&B28767 or microinjected with the recombinant proteins of the indicated mutants of RhoA or ROKα. The percentages of neurite-retracted cells were determined 30 min after the addition of the agonist or the microinjection of the proteins, as described under "Experimental Procedures". RhoA^{V14} or RhoA^{V14A37} was injected at 1 mg/ml, and CD-ROKα or CD-ROKα^{K112G} was injected at 2 mg/ml, respectively. Data are the mean ± S.E. of triplicate experiments.

Effects of the Rho-binding Domain and the PH Domain of ROKα on the EP3 Receptor-mediated Neurite Retraction

Next I microinjected RBD-ROKα or PHD-ROKα, which served as dominant negative forms of ROKα, into the differentiated cells and examined each effect on the M&B28767-induced neurite retraction. When the cells had been microinjected with RBD-ROKα or PHD-ROKα, the M&B28767-induced neurite retraction was inhibited (Fig. 1-6). All the cells microinjected with RBD-ROKα or PHD-ROKα had no response to M&B28767. These results suggest that ROKα is involved in

the EP3 receptor-mediated neurite retraction in the PC12 cells. Taken together, my results suggest that ROKα induces neurite retraction acting downstream of Rho in the NGF-differentiated PC12 cells.

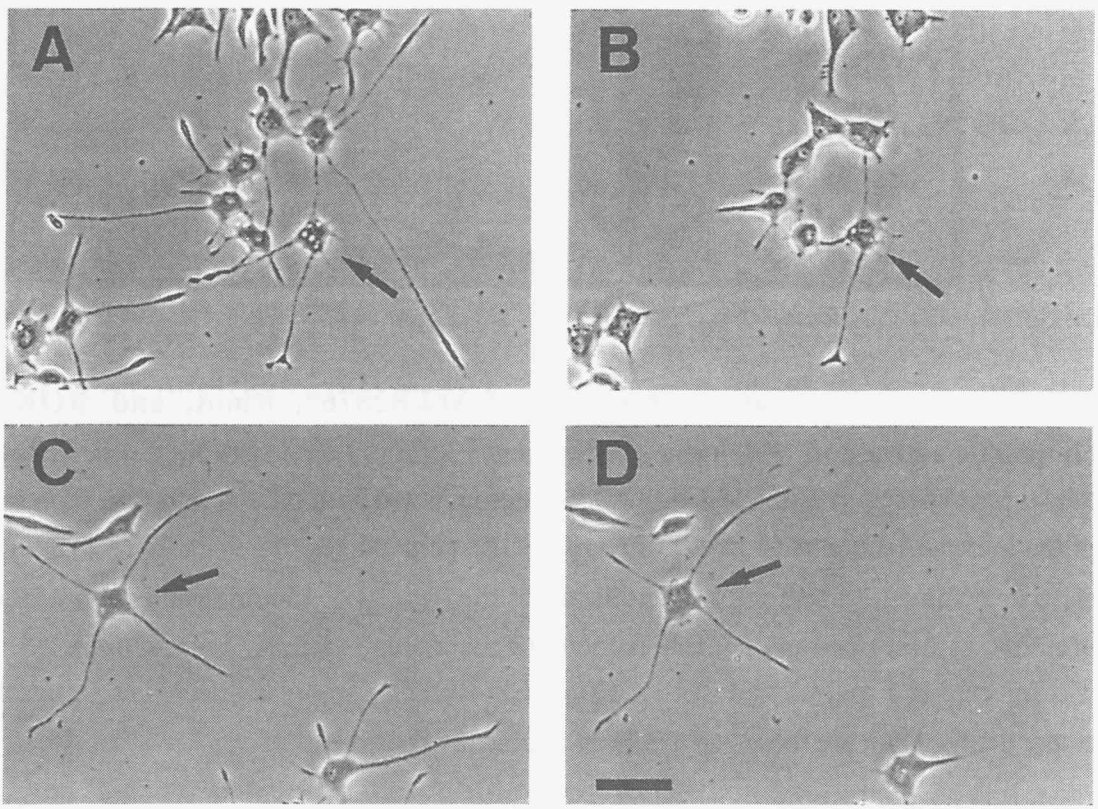

Figure 1-6. Effect of the Rho-binding domain and the PH domain of ROKα on M&B28767-induced neurite retraction. The NGF-differentiated cells were microinjected with 2 mg/ml of RBD-ROKα (*A* and *B*), or 1 mg/ml of PHD-ROKα (*C* and *D*), and photographed before (*A* and *C*) and 30 min after (*B* and *D*) addition of 1 μM M&B28767. The *arrows* indicate injected cells. The results shown are representative of three independent experiments. At least 20 cells were microinjected in each experiment, and all cells microinjected gave the described response. The *bar* represents 50 μm.

Discussion

In the present study, I have found that ROKα is involved in the receptor-mediated neurite retraction acting downstream of Rho in NGF-differentiated PC12 cells. Recently, ROKα was shown to be involved in Rho-induced formation of stress fibers and focal adhesion in other cell types such as fibroblasts. However, the organization of stress fibers induced by constitutively active ROKα was apparently different from that induced by lysophosphatidic acid or constitutively active Rho (28, 29), suggesting that additional signals were required for Rho-induced stress fiber formation. In this study, however, microinjection of CD-ROKα sufficiently induced neurite retraction similar to that induced by $RhoA^{V14}$ even though C3 exoenzyme had been preinjected, while CD-$ROK\alpha^{K112G}$ failed to induce neurite retraction (Figs. 1-4 and 1-5), suggesting that the increase in the kinase activity of ROKα by Rho appears to be sufficient for inducing neurite retraction. Since myosin-binding subunit of myosin phosphatase and MLC are known to be substrates for ROKα and activation of ROKα leads to phosphorylation and activation of myosin (26, 27), neurite retraction may be induced by ROKα-mediated regulation of myosin phosphorylation. In addition, it was recently reported that glial fibrillary acidic protein, an intermediate filament protein expressed in the cytoplasm of astroglia, was identified as another substrate for ROKα (33). Therefore, I will consider substrate(s) of this kinase for neurite retraction in future studies. Until now, we have obtained evidence that the activation of EP3 receptor, coupling to Rho activation, did not affect the NGF-induced MAP kinase activation in the PC12 cells (data not shown), suggesting that the activation of Rho or ROKα did not inhibit the NGF-induced signaling to

the Ras-MAP kinase pathway. To examine the direct effect of Rho or ROKα on the NGF-induced differentiation, I am currently establishing PC12 cell lines that express $RhoA^{V14}$ or CD-ROKα under the control of an inducible promoter.

As shown in Fig. 1-6, two fragments of ROKα, the Rho-binding domain and the PH domain served as dominant negative forms of ROKα in the EP3 receptor-mediated neurite retraction, as reported for the formation of stress fibers and focal adhesion (28, 29). ROKα has been shown to be translocated to peripheral membranes upon transfection with $RhoA^{V14}$ (21). Since PH domains are supposed to play a key role in localization of molecules to the specific target regions in the membranes, the PH domain of ROKα may localize this kinase at the specified region in response to the EP3 receptor-induced activation of Rho, and this translocation of ROKα to its target region seems to be essential for inducing neurite retraction. On the other hand, RBD-ROKα may block the interaction between endogenous Rho and ROKα. We also showed that $RhoA^{V14A37}$, a mutant at the effector region, lost the ability to induce neurite retraction in the differentiated PC12 cells (Fig. 1-1, *E* and *F*, and Fig. 1-5). Indeed, $RhoA^{V14}$ bound to the RBD-ROKα but $RhoA^{V14A37}$ did not (data not shown). This defect in binding to ROKα seems to be the reason for the inability of $RhoA^{V14A37}$ to induce neurite retraction.

In this study, I have shown that ROKα is an essential component of Rho-mediated neurite retraction in neuronal cells. Considering that ROKα is enriched in the brain (28) and expressed in neurons (34), ROKα may play a critical role in the regulation of neuronal cell morphology and axonal guidance in the nervous system.

2. Constitutively Active $G\alpha_{12}$, $G\alpha_{13}$, and $G\alpha_q$ Induce Rho-dependent Neurite Retraction through Different Signaling Pathways

Summary

In neuronal cells, activation of a certain heterotrimeric G protein-coupled receptor causes neurite retraction and cell rounding via small GTPase Rho. However, the specific heterotrimeric G proteins that mediate Rho-dependent neurite retraction and cell rounding have not yet been identified. Here I investigated the effects of expression of constitutively active Gα subunits on the morphology of differentiated PC12 cells. Expression of GTPase-deficient $G\alpha_{12}$, $G\alpha_{13}$, and $G\alpha_q$, but not $G\alpha_{i2}$, caused neurite retraction and cell rounding in differentiated PC12 cells. These morphological changes induced by $G\alpha_{12}$, $G\alpha_{13}$, and $G\alpha_q$ were completely inhibited by C3 exoenzyme, which specifically ADP-ribosyrates and inactivates Rho. A tyrosine kinase inhibitor tyrphostin A25 blocked the neurite retraction and cell rounding induced by $G\alpha_{13}$ and $G\alpha_q$. However, tyrphostin A25 failed to inhibit the $G\alpha_{12}$-induced neuronal morphological changes. On the other hand, inhibition of protein kinase C or elimination of extracellular Ca^{2+} blocked the neurite retraction and cell rounding induced by Gαq, whereas the morphological effects of $G\alpha_{12}$ and $G\alpha_{13}$ did not require activation of protein kinase C and extracellular Ca^{2+}. These results demonstrate that activation of $G\alpha_{12}$, $G\alpha_{13}$, and $G\alpha_q$ induces Rho-dependent morphological changes in PC12 cells through different signaling pathways.

Introduction

The activation of a certain heterotrimeric G protein-coupled receptor, such as LPA, sphingosine-1-phosphate and thrombin receptors, was shown to cause Rho-dependent neurite retraction in several neuronal cell lines (17, 18, 35). However, the heterotrimeric G proteins, which are coupled to those receptors for induction of neurite retraction, have not yet been identified. Previous studies demonstrated that pertussis toxin (PT) did not inhibit receptor-mediated neurite retraction (12, 36), indicating that this action was not mediated by G_i or G_o. Furthermore, the activation of G_s by cholera toxin or an elevation of cAMP by forskolin failed to induce neurite retraction but rather suppressed the receptor-mediated neurite retraction (31, 37), suggesting that G_s activation was not linked to induction of neurite retraction.

The G_{12} family of heterotrimeric G proteins, defined by $G\alpha_{12}$ and $G\alpha_{13}$, is the most recent family to be identified using a homology-based polymerase chain reaction (PCR) strategy (38, Fig. 2-1). Although immediate downstream effectors have not yet been identified, studies with the constitutively active mutants of $G\alpha_{12}$ and $G\alpha_{13}$ have resulted in the identification of several novel functions regulated by these $G\alpha$ subunits, including transformation of fibroblasts (39, 40), activation of the c-Jun N-terminal kinase cascade (41-43), stimulation of stress fiber formation and focal adhesion assembly (44, 45), stimulation of the Na^+-H^+ exchanger (46-48), the activation of phospholipase D (49), and the induction of apoptosis (50). These studies also indicate that the Ras or Rho family small GTPases appear to be involved in the downstream responses regulated by $G\alpha_{12}$ and $G\alpha_{13}$.

To investigate the role of the G_{12} family and other Gα subunits in neuronal cell morphology, I microinjected expression plasmids encoding GTPase-deficient mutants of Gα subunits into the nucleus of NGF-differentiated PC12 cells bearing neurites. In this study, I have shown that expression of constitutively active mutants of $G\alpha_{12}$, $G\alpha_{13}$, and $G\alpha_q$ cause Rho-dependent neurite retraction and cell rounding through different pathways.

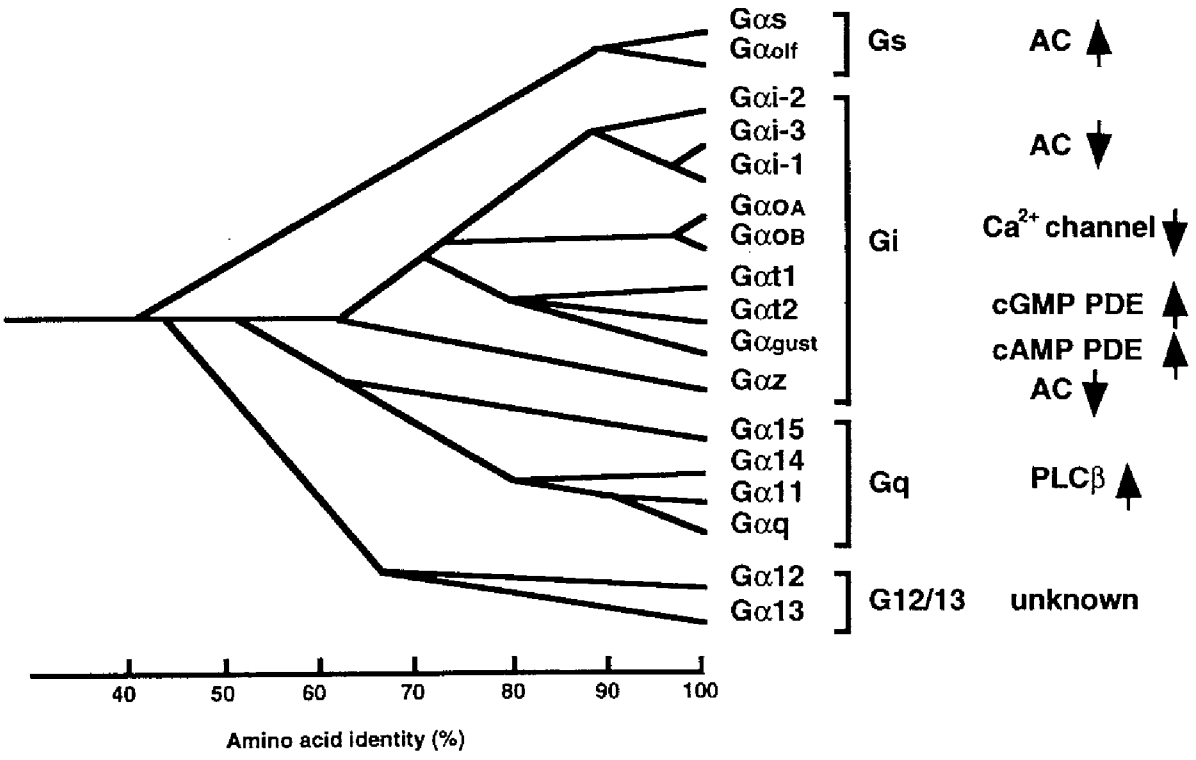

Fig. 2-1. Mammalian heterotrimeric G protein α subunits

Results

Expression of Constitutively Active Gα Subunits in NGF-differentiated PC12 Cells

To determine the role of the G_{12} family of heterotrimeric G proteins in neuronal cell morphology, I expressed constitutively active mutants of $G\alpha_{12}$ and $G\alpha_{13}$ in NGF-differentiated PC12 cells by nuclear microinjection of expression plasmids. Replacing a conserved glutamine

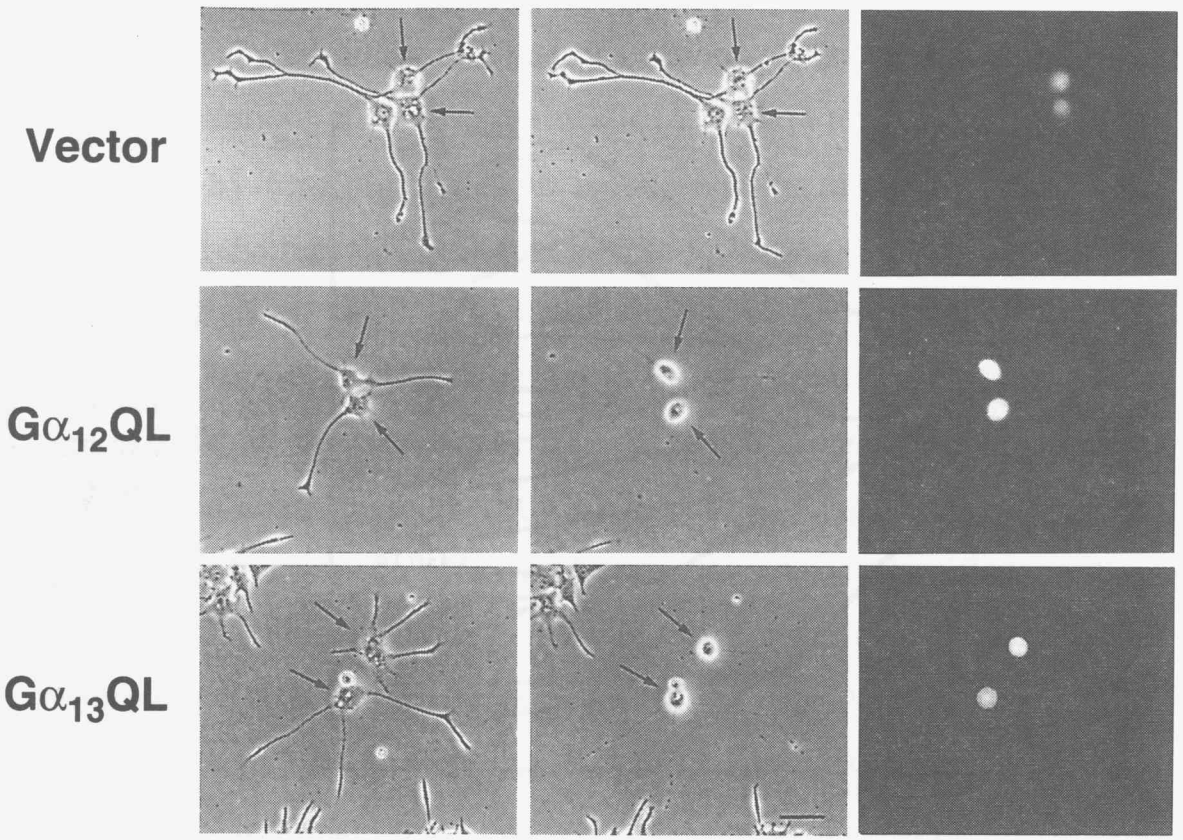

Figure 2-2. Neurite retraction and cell rounding induced by constitutively active $G\alpha_{12}$ and $G\alpha_{13}$. Expression plasmids (30 μg/ml) encoding $G\alpha_{12}$QL, $G\alpha_{13}$QL, or the empty vector (Vector) were microinjected into the nucleus of NGF-differentiated PC12 cells. Cells were photographed before (left panels) and 3 h after (middle panels) microinjection under the microscope with phase contrast, or by fluorescence of Texas red-coupled dextran co-microinjected with the expression vectors (right panels). The *arrows* indicate injected cells. The results shown are representative of three independent experiments. The *bar* represents 50 μm.

with a leucine in the G3 region of Gα subunit, which corresponds to residue 229 in $G\alpha_{12}$ or residue 226 in $G\alpha_{13}$, has been shown to result in a GTPase-deficient, constitutively active form of Gα subunit (51, 52). As shown in Fig. 2-2, microinjection of expression plasmids (30 μg/ml) encoding constitutively active $G\alpha_{12}$ ($G\alpha_{12}$Q229L; $G\alpha_{12}$QL) and $G\alpha_{13}$ ($G\alpha_{13}$Q226L; $G\alpha_{13}$QL) into the nucleus of NGF-differentiated PC12 cells caused retraction of their extended neurites and rounding of the cell body within 3 h. Cells microinjected with the empty vector did not exhibit any morphological changes, indicating that there were not any

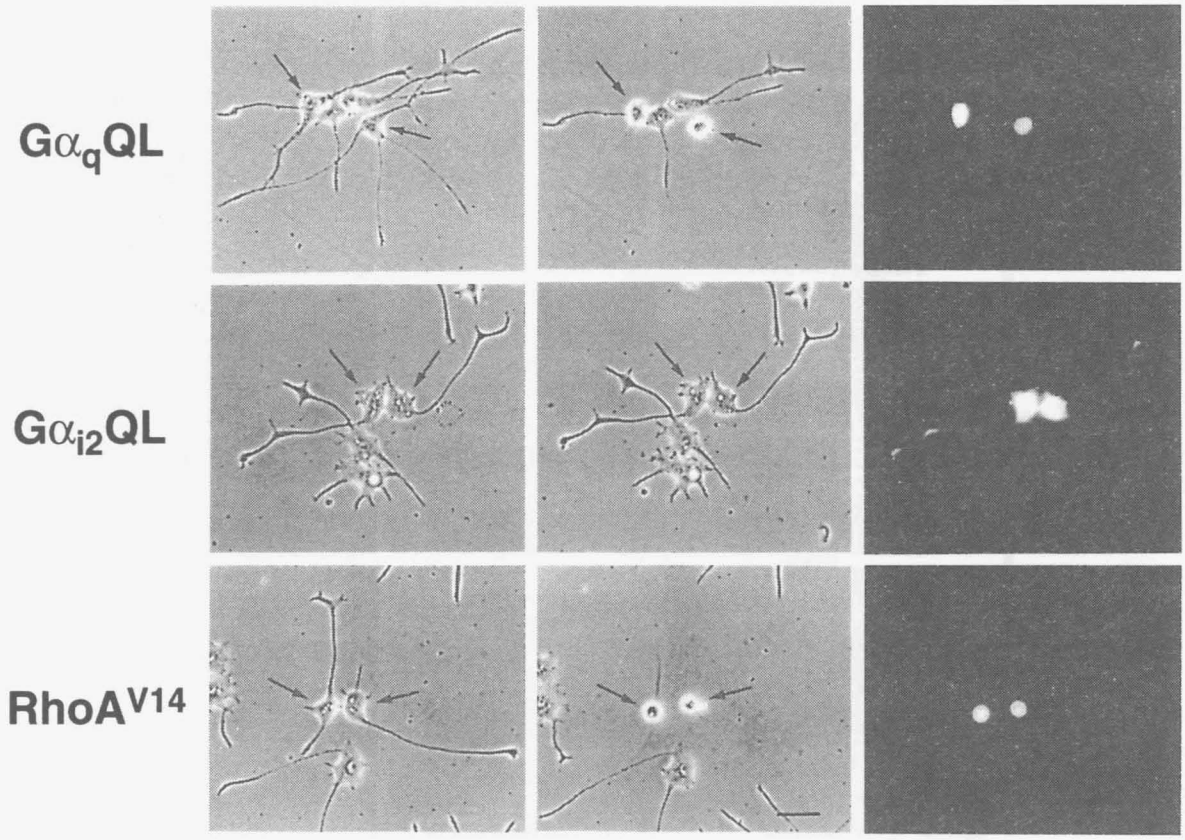

Figure 2-3. Neurite retraction and cell rounding induced by constitutively active $G\alpha_q$ and RhoA. Expression plasmids (30 μg/ml) encoding $G\alpha_qQL$, $G\alpha_{i2}QL$, or $RhoA^{V14}$ were microinjected into the nucleus of NGF-differentiated PC12 cells. Cells were photographed before (left panels) and 3 h after (middle panels) microinjection under the microscope with phase contrast, or by fluorescence of Texas red-coupled dextran co-microinjected with the expression vectors (right panels). The *arrows* indicate injected cells. The results shown are representative of three independent experiments. The *bar* represents 50 μm.

nonspecific effects due to nuclear microinjection itself. I also examined the effects of GTPase-deficient mutants of $G\alpha_q$ ($G\alpha_qQ209L$; $G\alpha_qQL$) and $G\alpha_{i2}$ ($G\alpha_{i2}Q205L$; $G\alpha_{i2}QL$) on differentiated PC12 cell morphology. As shown in Fig. 2-3, $G\alpha_qQL$, when expressed in differentiated PC12 cells, mimicked $G\alpha_{12}QL$ and $G\alpha_{13}QL$ in induction of neurite retraction and rounding of the cell body. In contrast, expression of $G\alpha_{i2}QL$ neither stimulated outgrowth nor caused retraction of neurites.

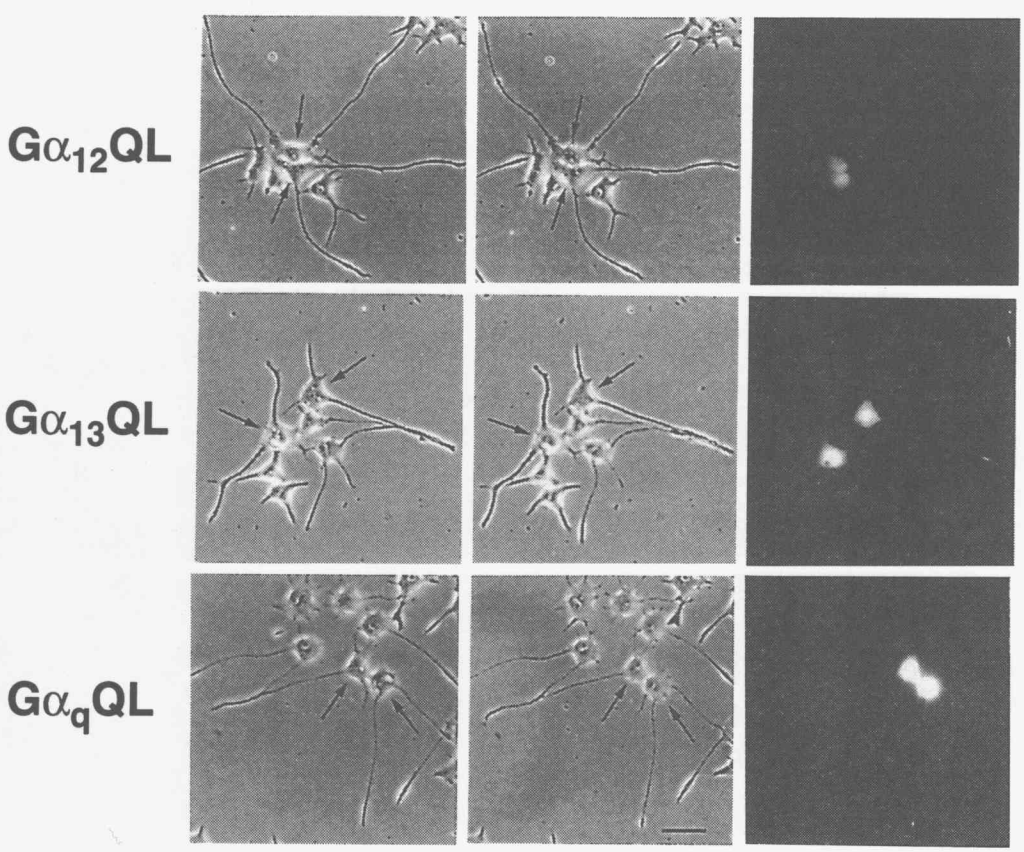

Figure 2-4. Effect of C3 exoenzyme on neuronal morphological changes induced by constitutively active Gα subunits. C3 exoenzyme (100 μg/ml) was co-microinjected with expression plasmids (30 μg/ml) encoding $G\alpha_{12}QL$, $G\alpha_{13}QL$, or $G\alpha_qQL$ into differentiated PC12 cells. Cells were photographed before (left panels) and 3 h after (middle panels) microinjection under the microscope with phase contrast, or by fluorescence of Texas red-coupled dextran co-microinjected with the expression vectors (right panels). The *arrows* indicate injected cells. The results shown are representative of three independent experiments. The *bar* represents 50 μm.

Effect of C3 Exoenzyme on Constitutively Active Gα Subunits-induced Neuronal Morphological Changes

Previous studies have shown that small GTPase Rho is required for neurite retraction in response to a certain G protein-coupled receptor agonist such as LPA (17, 18, 35). As shown in Fig. 2-3, microinjection of expression plasmids encoding a constitutively active form of RhoA, $RhoA^{V14}$, caused the retraction of neurites and rounding of the cell body. These morphological changes induced by $RhoA^{V14}$ were quite similar to those induced by $G\alpha_{12}QL$, $G\alpha_{13}QL$, and $G\alpha_qQL$ (Figs. 2-2 and 2-3). Therefore, to examine whether the neuronal morphological changes induced by constitutively active forms of Gα subunits were Rho-dependent, I co-microinjected the constitutively active Gα-encoding

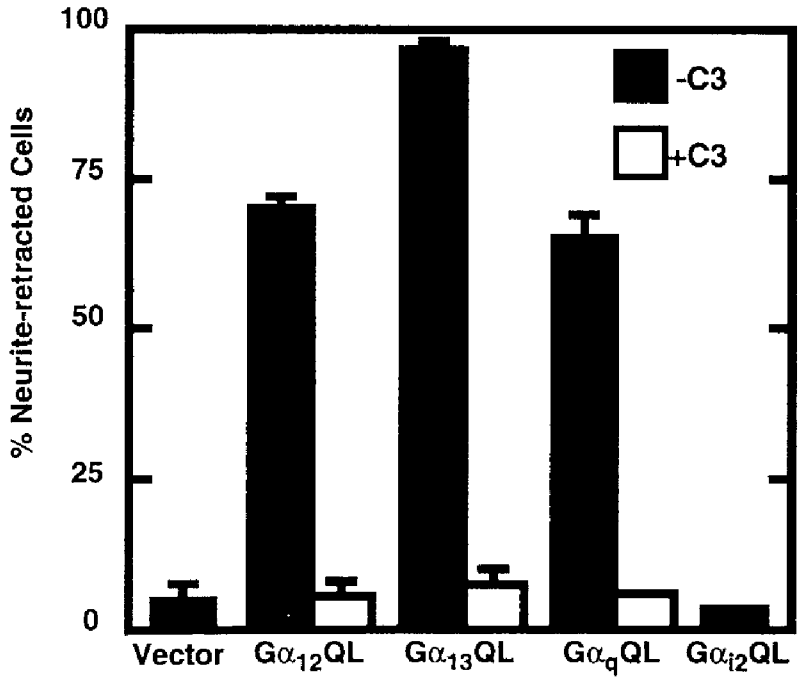

Figure 2-5. Quantification of effect of C3 exoenzyme on neurite retraction induced by constitutively active Gα subunits. Differentiated PC12 cells were microinjected with expression plasmids (30 μg/ml) encoding $G\alpha_{12}QL$, $G\alpha_{13}QL$, $G\alpha_qQL$, $G\alpha_{i2}QL$, or the empty vector (Vector) in the absence (-C3) or the presence (+C3) of 100 μg/ml C3 exoenzyme. The percentages of neurite-retracted cells were determined 3 h after microinjection as described under "Experimental Procedures". Data are the means ± S.E. of triplicate experiments.

plasmids into the cells with C3 exoenzyme. As shown in Figs. 2-4 and 2-5, co-microinjection of C3 exoenzyme (100 μg/ml) completely blocked both neurite retraction and cell rounding induced by $G\alpha_{12}QL$, $G\alpha_{13}QL$, and $G\alpha_qQL$. I also co-microinjected expression plasmids encoding dominant negative form of RhoA, $RhoA^{N19}$, into the cells with the constitutively active mutants of Gα subunits. Coexpression of $RhoA^{N19}$ slightly blocked neurite retraction induced by Gα subunits but was less effective than co-injection of C3 exoenzyme (data not shown). $RhoA^{N19}$ would not be an effective inhibitor for complete suppression of Gα subunits-induced morphological changes due to coexpression of $RhoA^{N19}$ and Gα subunits or requirement of large amount of $RhoA^{N19}$ for the suppression.

Effect of a Tyrosine Kinase Inhibitor Tyrphostin A25 on Neuronal Morphological Changes Induced by Constitutively Active Gα Subunits

A previous study showed that a tyrosine kinase inhibitor tyrphostin A25 inhibited stress fiber formation stimulated by LPA but not by microinjection of constitutively active Rho in quiescent Swiss 3T3 fibroblasts, indicating that a tyrosine kinase was involved in the LPA-stimulated stress fiber formation acting upstream of Rho (53). Therefore, I examined the effect of tyrphostin A25 on neuronal morphological changes induced by constitutively active Gα subunits. As shown in Figs. 2-6 and 2-7, treatment of differentiated cells with tyrphostin A25 (150 μM) inhibited the $G\alpha_{13}QL$- and $G\alpha_qQL$-induced neurite retraction and cell rounding. In contrast, the neurite retraction and cell rounding induced by $G\alpha_{12}QL$ were not influenced by this tyrosine kinase inhibitor. Thus, tyrphostin A25 specifically inhibited the signaling of $G\alpha_{13}QL$ and $G\alpha_qQL$. In addition, I examined the effect of another tyrosine kinase inhibitor tyrphostin AG1478 on

morphological changes induced by constitutively active Gα subunits. Treatment of differentiated cells with tyrphostin AG1478 (10 μM) also specifically inhibited the $G\alpha_{13}QL$- and $G\alpha_qQL$-induced neurite retraction and cell rounding, and $G\alpha_{12}QL$-induced morphological changes were not inhibited by this inhibitor (data not shown).

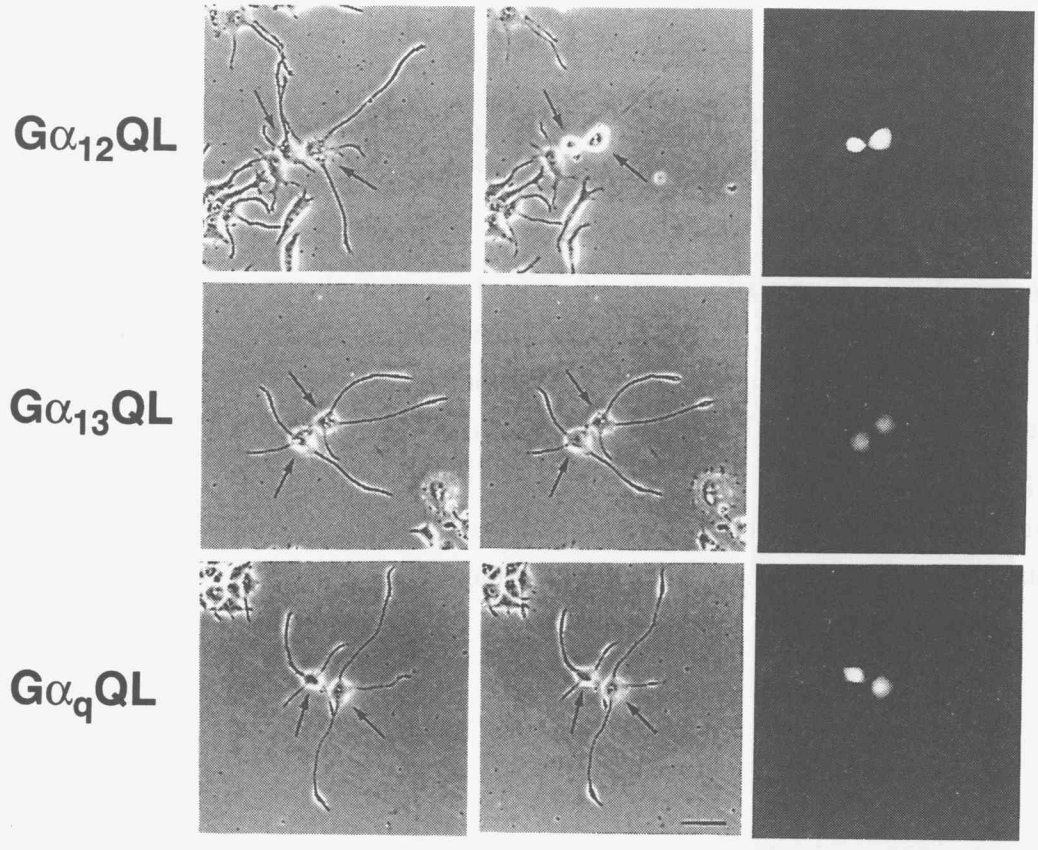

Figure 2-6. Effect of tyrphostin A25 on neuronal morphological changes induced by constitutively active Gα subunits. After differentiated PC12 cells had been microinjected with expression plasmids (30 μg/ml) encoding $G\alpha_{12}QL$, $G\alpha_{13}QL$, $G\alpha_qQL$, they were incubated with tyrphostin A25 (150 μM) for 3 h. Cells were photographed before (left panels) and 3 h after (middle panels) microinjection under the microscope with phase contrast, or by fluorescence of Texas red-coupled dextran co-microinjected with the expression vectors (right panels). The *arrows* indicate injected cells. The results shown are representative of three independent experiments. The *bar* represents 50 μm.

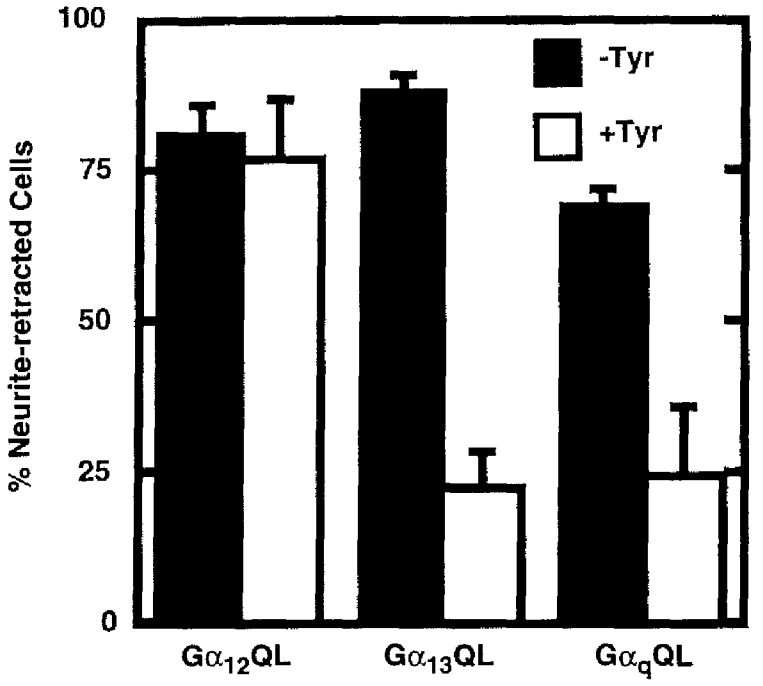

Figure 2-7. Quantification of effect of tyrphostin A25 on neurite retraction induced by constitutively active Gα subunits. After differentiated PC12 cells had been microinjected with expression plasmids (30 μg/ml) encoding $G\alpha_{12}QL$, $G\alpha_{13}QL$, or $G\alpha_qQL$, they were incubated with vehicle (-Tyr) or 150 μM tyrphostin A25 (+Tyr) for 3 h. The percentages of neurite-retracted cells were determined 3 h after microinjection as described under "Experimental Procedures". Data are the means ± S.E. of triplicate experiments.

Effects of Protein Kinase C Inhibition and Elimination of Extracellular Ca^{2+} on Neuronal Morphological Changes Induced by Constitutively Active Gα Subunits

A number of the cellular responses caused by activation of $G\alpha_q$ have been shown to be mediated by activation of protein kinase C (PKC) or elevation of intracellular Ca^{2+} concentration. Therefore, I examined whether activation of PKC was required for neuronal morphological changes induced by constitutively active $G\alpha_q$ and $G\alpha_{12}/G\alpha_{13}$. Exposing

PC12 cells to 12-*O*-tetradecanoylphorbol-13-acetate (TPA) for more than 24 h has been reported to induce down-regulation of PKC (54). As shown in Figs. 2-8 and 2-10, down-regulation of endogenous PKC by 24-h exposure to 1 μM TPA diminished the amount of neurite-retracted cells caused by $G\alpha_qQL$, whereas the $G\alpha_{12}QL$- and $G\alpha_{13}QL$-induced morphological changes were not significantly altered by PKC depletion from cells. Similar results were obtained in the treatment of cells with the PKC inhibitor Ro31-8220 (300 nM) (Fig. 2-10). These results

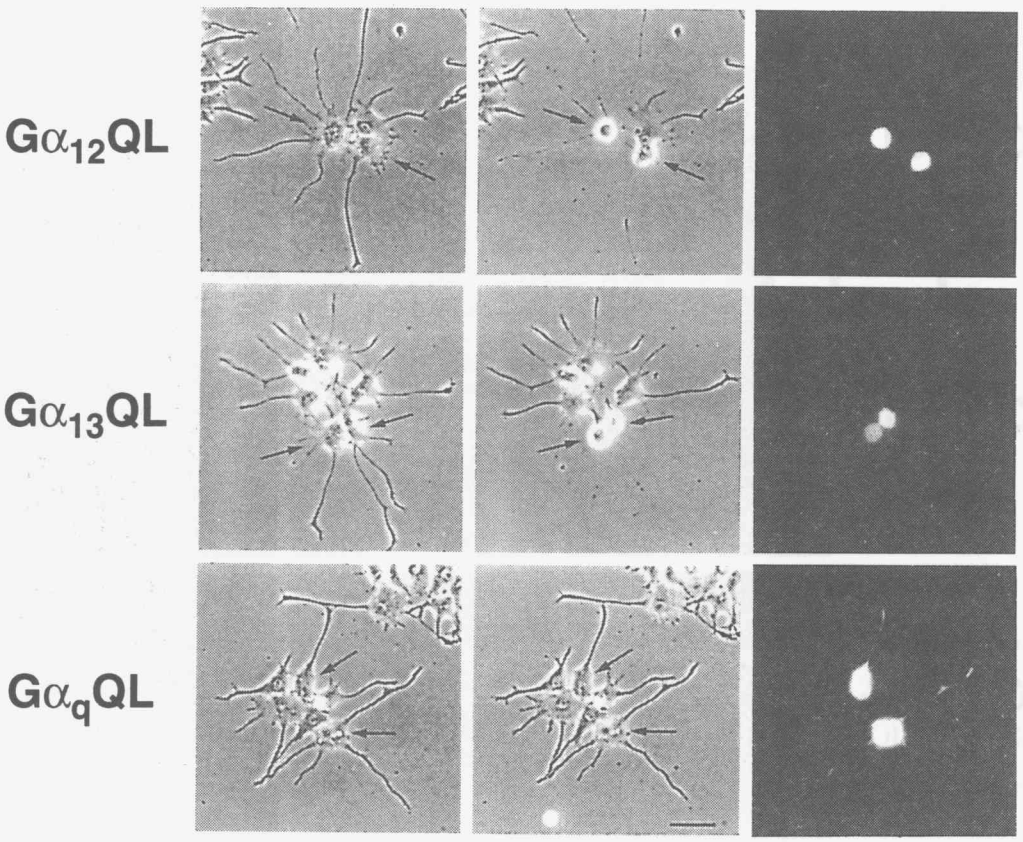

Figure 2-8. Effect of depletion of intracellular PKC on neuronal morphological changes induced by constitutively active Gα subunits. Differentiated PC12 cells, which had been pretreated with TPA (1 μM) for 24 h, were microinjected with expression plasmids (30 μg/ml) encoding $G\alpha_{12}QL$, $G\alpha_{13}QL$, $G\alpha_qQL$. Cells were photographed before (left panels) and 3 h after (middle panels) microinjection under the microscope with phase contrast, or by fluorescence of Texas red-coupled dextran co-microinjected with the expression vectors (right panels). The *arrows* indicate injected cells. The results shown are representative of three independent experiments. The *bar* represents 50 μm.

indicate that inhibition of PKC activity specifically interferes with the signaling pathway of $G\alpha_q$ for neurite retraction and cell rounding.

Next I examined the role of Ca^{2+} signaling in neuronal morphological changes induced by activated Gα subunits. Differentiated PC12 cells were incubated in a Ca^{2+}-free medium in the presence of 2 mM EGTA during expression of Gα subunits. Under these conditions, expression of $G\alpha_qQL$ failed to induce neurite retraction and cell rounding. In contrast, neuronal morphological

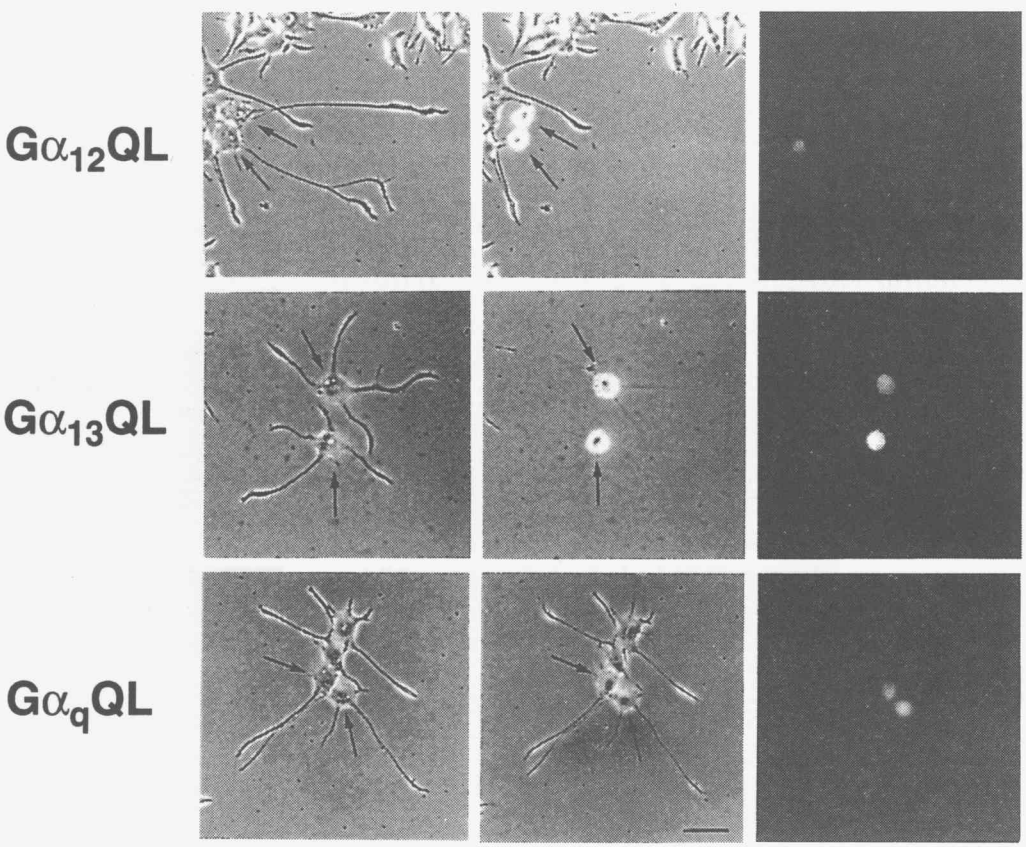

Figure 2-9. Effect of elimination of extracellular Ca^{2+} on neuronal morphological changes induced by constitutively active Gα subunits. After differentiated PC12 cells had been microinjected with expression plasmids (30 μg/ml) encoding $G\alpha_{12}QL$, $G\alpha_{13}QL$, $G\alpha_qQL$, they were incubated in the Ca^{2+}-free medium containing EGTA (2 mM) for 3 h. Cells were photographed before (left panels) and 3 h after (middle panels) microinjection under the microscope with phase contrast, or by fluorescence of Texas red-coupled dextran co-microinjected with the expression vectors (right panels). The *arrows* indicate injected cells. The results shown are representative of three independent experiments. The *bar* represents 50 μm.

changes induced by $G\alpha_{12}QL$ and $G\alpha_{13}QL$ were normally occurred in a Ca^{2+}-free medium with EGTA (Figs. 2-9 and 2-10). These results indicate that Ca^{2+} influx is required for the $G\alpha_qQL$-induced neuronal morphological changes.

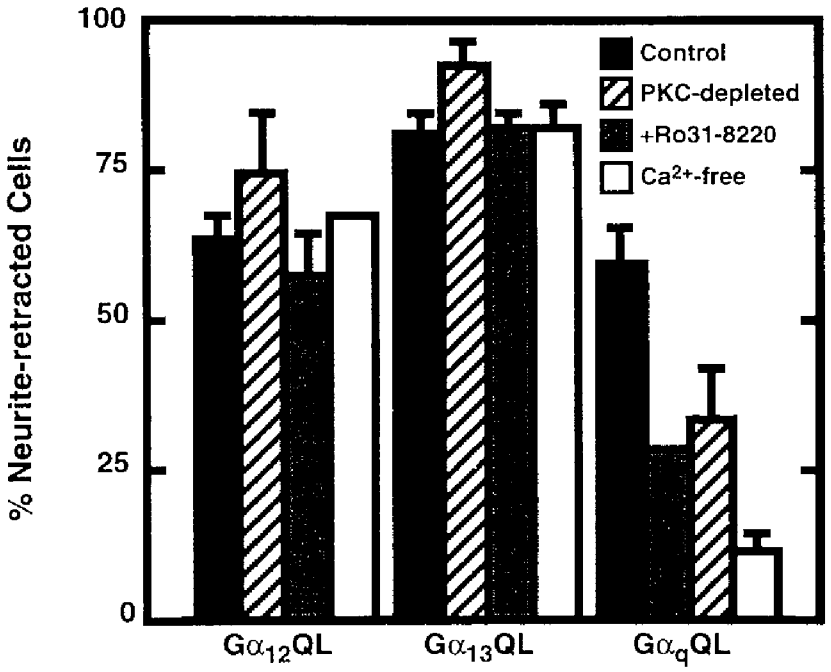

Figure 2-10. Quantification of effects of inhibition of PKC and elimination of extracellular Ca^{2+} on neurite retraction induced by constitutively active Gα subunits. After differentiated PC12 cells had been microinjected with expression plasmids (30 μg/ml) encoding $G\alpha_{12}QL$, $G\alpha_{13}QL$, or $G\alpha_qQL$, they were incubated in the absence (Control) or the presence of 300 nM Ro31-8220 (+Ro31-8220), or in the Ca^{2+}-free medium containing 2 mM EGTA (Ca^{2+}-free) for 3 h. Or expression plasmids were microinjected into differentiated cells which had been treated with 1 μM TPA for 24 h before microinjection to induce down-regulation of endogenous PKC (PKC-depleted). The percentages of neurite-retracted cells were determined 3 h after microinjection as described under "Experimental Procedures". Data are the means ± S.E. of triplicate experiments.

Discussion

Activation of a certain G protein-coupled receptor has been reported to induce Rho-dependent neurite retraction and cell rounding in neuronal cell lines (17, 18, 31, 35). Here I have demonstrated that constitutively active forms of $G\alpha_{12}$, $G\alpha_{13}$, and $G\alpha_q$, but not $G\alpha_{i2}$, can trigger neurite retraction and cell rounding in NGF-differentiated PC12 cells. These morphological changes were similar to those induced by constitutively active RhoA, $RhoA^{V14}$ (Fig. 2-3), and C3 exoenzyme, which specifically ADP-ribosyrates and inactivates Rho (15, 16), completely inhibited both neurite retraction and cell rounding induced by $G\alpha_{12}QL$, $G\alpha_{13}QL$, and $G\alpha_qQL$ (Figs. 2-4 and 2-5), indicating that activation of $G\alpha_{12}$, $G\alpha_{13}$, and $G\alpha_q$ induces neurite retraction and cell rounding through a Rho-dependent signaling pathway in differentiated PC12 cells.

$G\alpha_{12}$ and $G\alpha_{13}$, the members of the G_{12} class of heterotrimeric G protein, show a 67% amino acid identity with each other, and often cause similar responses in various cell types, including transformation of fibroblasts, activation of the c-Jun N-terminal kinase cascade, and stimulation of stress fiber formation and focal adhesion assembly (55). I have also shown that both $G\alpha_{12}$ and $G\alpha_{13}$ can trigger Rho-dependent neurite retraction and cell rounding. These findings suggest that $G\alpha_{12}$ and $G\alpha_{13}$ may interact with a common effector. In this study, however, the tyrosine kinase inhibitor tyrphostin A25 blocked the $G\alpha_{13}QL$-induced neurite retraction and cell rounding, whereas the $G\alpha_{12}QL$-induced morphological changes were not influenced by this tyrosine kinase inhibitor (Figs. 2-6 and 2-7), indicating that a tyrphostin-sensitive tyrosine kinase was involved in the signaling of $G\alpha_{13}$ but not in that of

$G\alpha_{12}$. This finding strongly suggests that $G\alpha_{12}$ and $G\alpha_{13}$ use different signaling pathways to regulate neuronal cell morphology. The differences in the sensitivity to tyrphostin between $G\alpha_{12}$ and $G\alpha_{13}$ were also shown in the signaling of $G\alpha_{12}$- and $G\alpha_{13}$-stimulated stress fiber formation and focal adhesion assembly in Swiss 3T3 fibroblasts (45). Furthermore, it was previously reported that $G\alpha_{12}$ and $G\alpha_{13}$ stimulated Na^+-H^+ exchangers through different mechanisms in COS-7 cells (56, 57). Therefore, it is likely that $G\alpha_{12}$ and $G\alpha_{13}$ activate different effectors to regulate their cellular functions.

Activation of $G\alpha_q$ can stimulate the family of phospholipase C (PLC)-β, which results in stimulation of PKC activity and elevation of intracellular Ca^{2+} concentration. In this study, both depletion of endogenous PKC by TPA and the PKC inhibitor Ro31-8220 specifically diminished the amount of neurite-retracted cells induced by $G\alpha_qQL$, whereas the $G\alpha_{12}QL$- and $G\alpha_{13}QL$-induced morphological changes were not influenced (Figs. 2-8 and 2-10). In addition, elimination of extracellular Ca^{2+} also inhibited the effects of $G\alpha_qQL$ but not those of $G\alpha_{12}QL$ and $G\alpha_{13}QL$ (Figs. 2-9 and 2-10). It has been known that inositol 1,4,5-trisphosphate and inositol 1,3,4,5-tetrakisphosphate, products of PLC activation pathways, activate Ca^{2+}-permeable channels in plasma membranes (58, 59). Recently, $G\alpha_q$ was reported to activate inositol 1,4,5-trisphosphate-operated Ca^{2+}-permeable channels (60). The requirement of extracellular Ca^{2+} for the $G\alpha_q$-induced morphological changes could be interpreted by this $G\alpha_q$-mediated Ca^{2+}-permeable channel activation. Therefore, both PKC activation and Ca^{2+} influx are essential elements in the signaling of $G\alpha_q$ upstream of Rho. I also examined the involvement of PLC in the $G\alpha_qQL$ signaling using a PLC inhibitor U-73122, but this compound was cytotoxic for differentiated PC12 cells, and treatment with U-73122 alone caused cell

detachment. Interestingly, both PKC activity and Ca^{2+} influx as a result of PLC activation appeared to be required for LPA-induced neurite retraction in NGF-differentiated PC12 cells (18). Therefore, it is likely that a G_q-coupled LPA receptor stimulates PLC activity and resultant activation of PKC and Ca^{2+} influx induces Rho-dependent neurite retraction in PC12 cells.

Interestingly, the $G\alpha_qQL$-induced neurite retraction and cell rounding were also blocked by treatment of cells with the tyrosine kinase inhibitor tyrphostin A25 (Figs. 2-6 and 2-7), indicating that a tyrphostin-sensitive tyrosine kinase is involved in the signaling from $G\alpha_q$ to Rho. My present study did not show whether this tyrphostin-sensitive tyrosine kinase acts upstream or downstream of Ca^{2+} and PKC in the signaling from $G\alpha_q$ to Rho. Since activation of $G\alpha_q$ can directly stimulate PLC which results in stimulation of PKC activity and elevation of intracellular Ca^{2+} concentration, this tyrphostin-sensitive tyrosine kinase may act downstream of Ca^{2+} and PKC. Recently, a novel nonreceptor tyrosine kinase PYK2 has been shown to mediate G_q-coupled receptor-stimulated activation of MAP kinase cascade in PC12 cells, and the activity of this tyrosine kinase appears to be regulated by the elevation of the intracellular Ca^{2+} concentration as well as by PKC activation (61). Therefore, PYK2 can be speculated to be a candidate for the tyrosine kinase, which links the signal of $G\alpha_q$ to Rho for the induction of neurite retraction and cell rounding. A tyrphostin-sensitive tyrosine kinase was of course involved in the signaling of $G\alpha_{13}$ to Rho. However, in contrast to $G\alpha_q$, $G\alpha_{13}$ did not require either PKC activation or Ca^{2+} influx. Two potential explanations for the difference between signaling pathways of $G\alpha_{13}$ and $G\alpha_q$ can be presented. One explanation is that an identical tyrosine kinase mediates the signals of $G\alpha_{13}$ and $G\alpha_q$ to Rho, but the pathways of both α subunits to activate

the tyrosine kinase are different; $G\alpha_q$ activates the kinase through PKC and Ca^{2+} influx while $G\alpha_{13}$ activates the kinase independent of PKC. The other explanation is that different tyrosine kinases are involved in the pathways of both α subunits. Further investigations are necessary to understand the signaling pathways from Gα subunits to Rho in neuronal cells.

Expression of a GTPase-deficient form of $G\alpha_q$ in undifferentiated PC12 cells was recently shown to induce neurite outgrowth during 2-3 weeks using the retrovirus-mediated infection procedure (62). In contrast, my results showed that expression of $G\alpha_q$QL in NGF-differentiated PC12 cells triggered neurite retraction within 3 h after microinjection. Therefore, these opposite effects of $G\alpha_q$ on the regulation of neurites may be due to different condition of cells in differentiation or different time scale for examination of morphological effects.

The data presented here demonstrated that constitutively active mutants of $G\alpha_{12}$, $G\alpha_{13}$, and $G\alpha_q$ can induce neurite retraction and cell rounding through different signaling pathways which, however, finally converge at activation of Rho. Rho, like other small GTPases, functions as a molecular switch; it is active in its GTP-bound state and inactive in its GDP-bound state. Upstream activation of the cycle is mediated by GEFs, which promote the exchange of GDP for GTP (Fig. 0-1). A number of putative GEFs for Rho and other Rho family GTPases have been identified, and some of these demonstrate Rho-specific GEF activity in vitro, including Lbc, Lfc, and Lsc (6, 63-65). In addition, they appear to be expressed in the same cell type (64). Therefore, one possibility for the existence of multiple GEFs for Rho in the same cell type may be related to the existence of different signaling pathways from Gα subunits to activation of Rho.

Recent studies have shown the involvement of the Rho family of small GTPases in the regulation of neurite outgrowth in primary neurons (66, 67). In embryonic chick dorsal root ganglion, inhibition of Rho with C3 exoenzyme stimulated the outgrowth of neurites (66), suggesting that activation of Rho suppresses neurite outgrowth in primary neurons. Therefore, $G\alpha_{12}$, $G\alpha_{13}$, and $G\alpha_q$ may play a negative regulator for neurite outgrowth through activation of Rho in primary neurons.

In this study, I have shown that activation of $G\alpha_{12}$, $G\alpha_{13}$, and $G\alpha_q$ can trigger Rho-dependent neurite retraction and cell rounding in differentiated PC12 cells through different signaling pathways. This study will contribute to the understanding of the signal transduction between heterotrimeric G protein-coupled receptors and Rho in neuronal cells.

3. Prostaglandin EP3 Receptor Induces Neurite Retraction through Small GTPase Rho

Summary

Prostaglandin EP3 receptor is widely distributed in the nervous system and is specifically localized to neurons, suggesting that EP3 receptor plays important roles in the nervous system. I established a PC12 cell line which stably expresses the EP3B receptor isoform isolated from bovine adrenal chromaffin cells and examined the effect of agonist stimulation on the neuronal morphology of the PC12 cells. In the differentiated cells, M&B28767, an EP3 agonist, caused neurite retraction in a PT-insensitive manner. *Clostridium botulinum* C3 exoenzyme completely inhibited the EP3 receptor-induced neurite retraction when microinjected into the cells, indicating that the morphological effect of the EP3 receptor is dependent on Rho activity. The EP3 receptor-mediated neurite retraction occurred normally in the PKC-down-regulated cells. Similar to the $G\alpha_{13}QL$-induced neurite retraction, tyrphostin A25, a tyrosine kinase inhibitor, blocked neurite retraction induced by activation of the EP3 receptor. These results indicate that the EP3 receptor is coupled to G_{13}, stimulating Rho-mediated neurite retraction.

Introduction

Prostaglandin (PG) E_2 is synthesized via cyclooxygenase pathway from arachidonic acid by a variety of cells in response to various physiological or pathological stimuli (Fig. 3-1). PGE_2 is one of the major PGs synthesized in the nervous system (68), and it has several important functions in the nervous system, such as generation of fever (69, 70), regulation of luteinizing hormone-releasing hormone secretion (71), pain modulation (72), and regulation of neurotransmitter release (73, 74). Although cyclooxygenase products including PGE_2 have been suggested to be involved in regulation of memory consolidation (75), the biological significance of PGE_2 in synaptic plasticity is not yet understood.

PGE_2 acts on cell surface receptors to exert its actions (76). PGE receptors are pharmacologically divided into four subtypes, EP1, EP2, EP3 and EP4, on the basis of their responses to various agonists and antagonists (77, 78). Among these subtypes, EP3 receptor has been most well characterized and has been suggested to be involved in such PGE_2 actions as contraction of the uterus (79), inhibition of gastric acid secretion (80), modulation of the neurotransmitter release (81), lipolysis in adipose tissue (82), and sodium and water reabsorption in the kidney tubules (83). Although the well-known EP3 receptor-mediated actions, mentioned above, are believed to be mediated through inhibition of adenylate cyclase by activation of Gi, coupling of EP3 receptors to other signal transduction pathways has been suggested (84, 85). The four subtypes of mouse PGE receptors have been cloned and it is demonstrated that they are heterotrimeric G protein-coupled rhodopsin-type receptors (86-89). Among these subtypes, the EP3 receptor was

most abundant in the brain and was specifically localized to neurons (90, 91).

To assess the role of the EP3 receptors in the nervous system, I introduced the cDNA for the EP3B receptor, one of the EP3 receptor isoforms isolated from bovine adrenal medulla (85), into PC12 cells. In this study, I have shown that the activation of the EP3 receptor causes neurite retraction through small GTPase Rho and that a tyrosine kinase is involved in the EP3 receptor-mediated neurite retraction acting upstream of Rho.

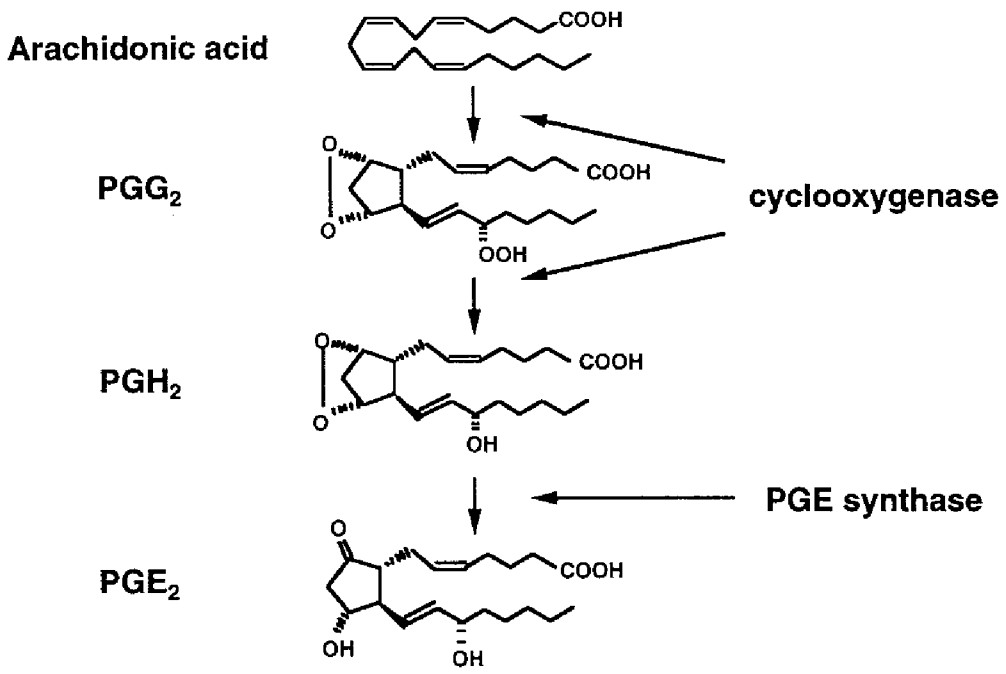

Fig. 3-1. Biosynthesis of PGE_2.

Results

Effect of M&B28767 on Morphology of the EP3 Receptor-Expressing PC12 Cells, Differentiated with NGF

To assess the role of EP3 receptors in neuronal morphology, I established PC12 cells, which stably expressed the EP3B receptor (151 fmol/mg protein). I initially examined the coupling.of the EP3 receptor to the classical signal transduction pathways, the adenylate cyclase and Ca^{2+} mobilization pathways. In these cells, the EP3 receptor inhibited

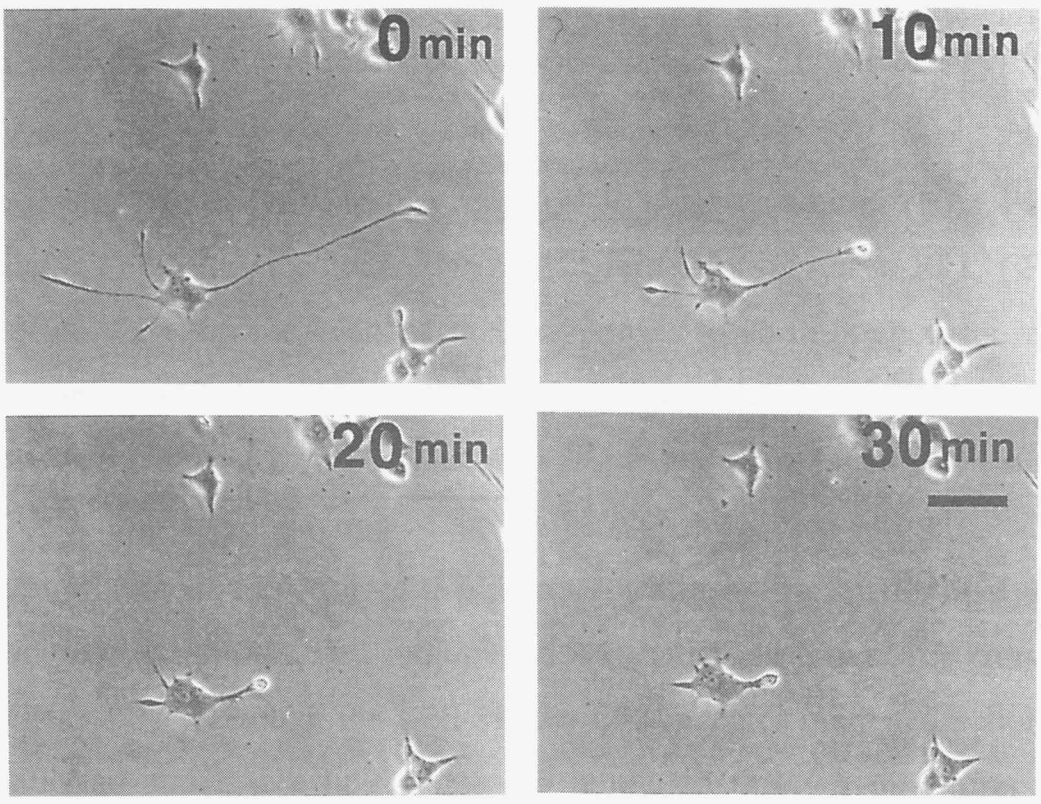

Figure 3-2. M&B28767-induced neurite retraction in EP3B receptor-expressing PC12 cells. After the cells had been differentiated for 5 d with NGF, 1 μM M&B28767 was added to the cells and they were photographed at the times indicated as described under "Experimental Procedures". The result shown is representative of three independent experiments that yielded similar results. Bar represents 50 μm.

adenylate cyclase activity through a PT-sensitive heterotrimeric G protein, but the receptor could not stimulate adenylate cyclase, phosphatidylinositol hydrolysis, or Ca^{2+} mobilization (data not shown), suggesting that the EP3 receptor is coupled to Gi, but not to Gs or Gq. I next examined the effect of M&B28767, a specific EP3 agonist, on the neuronal morphology of the EP3 receptor-expressing PC12 cells. As shown in Fig. 3-2, treatment of the cells with NGF induced neurite outgrowth. Addition of M&B28767 caused a dramatic morphological change in the NGF-differentiated PC12 cells. Within 10 min of the addition of the agonist neurites began to retract, and within 30 min, most neurites had retracted completely. Fig. 3-3*A* shows the time course of the effect of the agonist on neurite length. The neurite length became half of the original length within 20 min. The rate of neurite

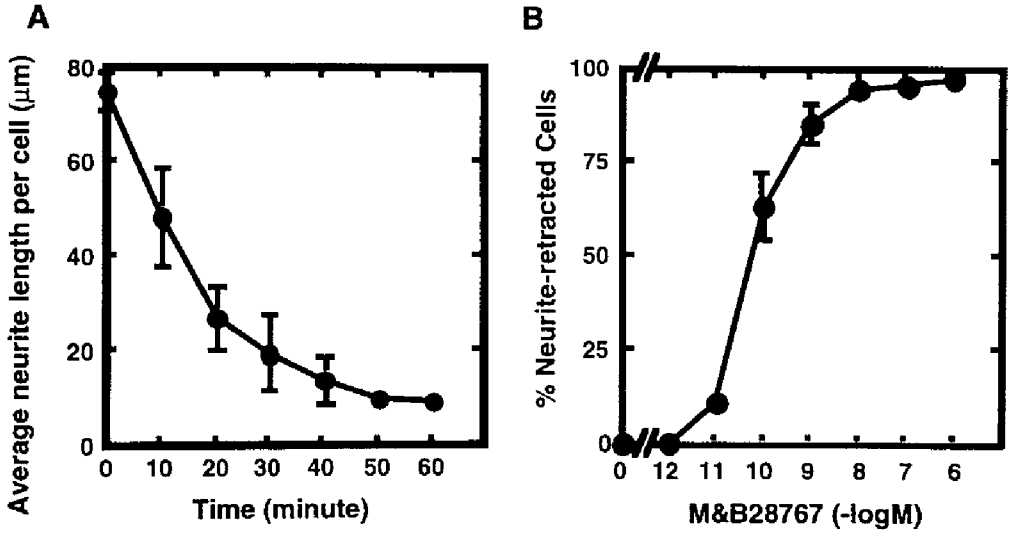

Figure 3-3. The time course and concentration dependency of M&B28767-induced neurite retraction. (*A*) Time course. After cells had been differentiated with NGF for 5 d, 1 μM M&B28767 was added. The average neurite length at the times indicated was measured as described in the Experimental Procedures. Data are means ± S.E. of triplicate experiments. (*B*) Concentration dependency. The differentiated cells were exposed to the indicated concentrations of M&B28767 for 60 min. The percentage of neurite retracted cells was determined as described in the Experimental Procedures. Data are means ± S.E. of triplicate experiments.

retraction was not dependent on the concentration of the agonist (data not shown). M&B28767 concentration-dependently increased the population of neurite retracted cells, and more than 90% of the total cells responded to 1 μM M&B28767 (Fig. 3-3*B*). However, a few cells resisted even high concentrations of the agonist. M&B28767-induced neurite retraction was not seen for more than 60 min in the untransfected cells (data not shown).

The EP3 receptor inhibited adenylate cyclase via a PT-sensitive heterotrimeric G protein. However, pretreating the EP3 receptor-expressing cells with PT for 12 h did not affect M&B28767-induced

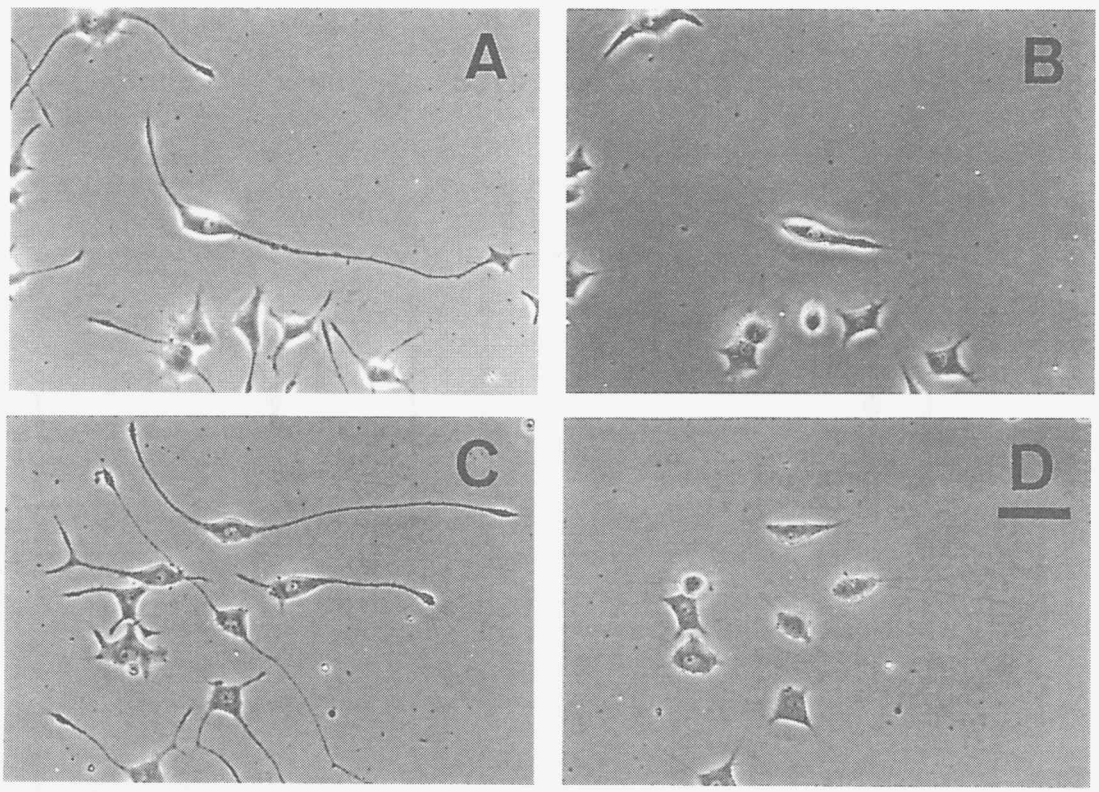

Figure 3-4. Effect of PT on M&B28767-induced neurite retraction. (*A*) Cells were differentiated with NGF for 5 d. (*B*) Cells in *A* were exposed to 1 μM M&B28767 for 60 min. (*C*) NGF-differentiated cells were treated with 20 ng/ml PT for 12 h. (*D*) Cells in *C* were exposed to 1 μM M&B28767 for 60 min. The results shown are representative of three independent experiments that yielded similar results. Bar represents 50 μm.

neurite retraction (Fig. 3-4 and 3-8), indicating that the EP3 receptor-mediated neurite retraction was not mediated through a PT-sensitive G protein.

I further examined the effect of protein kinase A (PKA) activation on the EP3 receptor-mediated neurite retraction. As shown in Fig. 3-5, whereas dibutyryl cAMP (Bt_2cAMP) did not affect the morphology of the differentiated cells, it strongly prevented M&B28767-induced neurite retraction. Fig. 3-8 shows the quantitative examination of the effect of Bt_2cAMP. It decreased the percentage of neurite-retracted cells in response to M&B28767 from 93.9% to 13.4%. These results

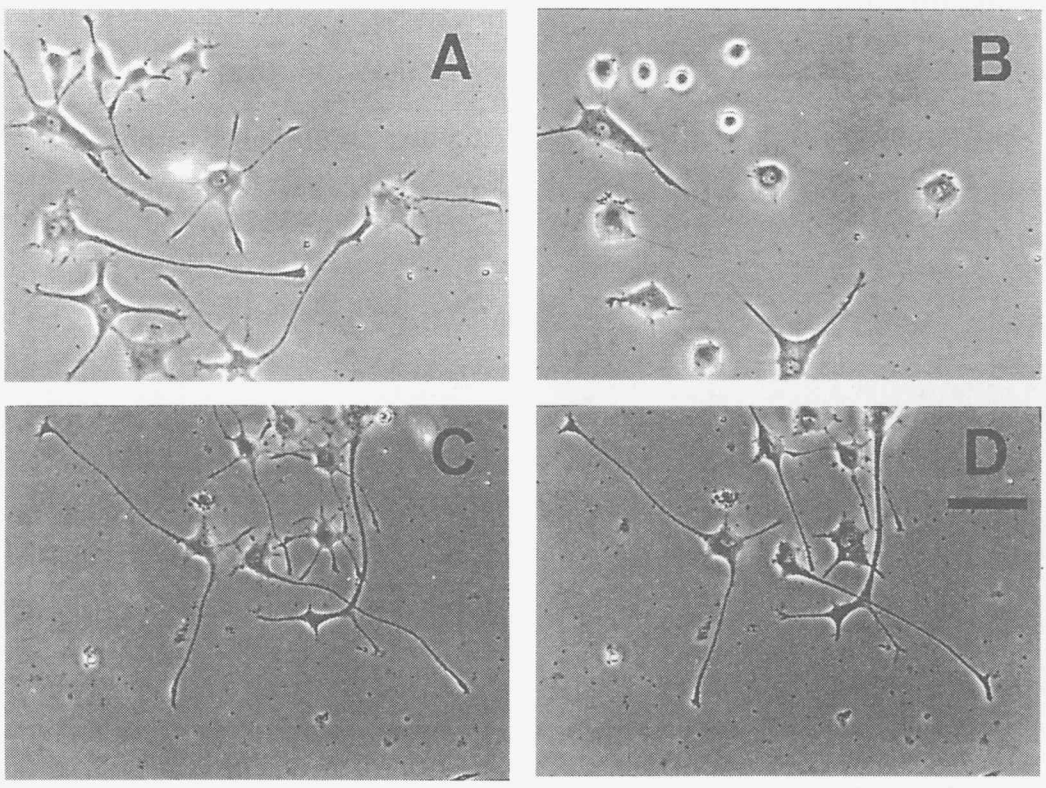

Figure 3-5. Effect of Bt_2cAMP on M&B28767-induced neurite retraction. (*A*) Cells were differentiated with NGF for 5 d. (*B*) Cells in *A* were exposed to 1 μM M&B28767 for 60 min. (*C*) Differentiated cells were pretreated with 500 μM Bt_2cAMP for 15 min. (*D*) Cells in *C* were exposed to 1 μM M&B28767 for 60 min. The results shown are representative of three independent experiments that yielded similar results. Bar represents 50 μm.

indicate that the activation of PKA suppresses EP3 receptor-mediated neurite retraction.

Effect of C3 Exoenzyme on M&B28767-induced Neurite Retraction

A small G protein, Rho, appears to be required for the retraction of neurites (17). To evaluate the participation of Rho in the EP3 receptor-mediated neurite retraction, the cells were microinjected with *C. botulinum* C3 exoenzyme, which specifically ADP-ribosylates Rho and suppresses the actions of Rho (15, 16). As shown in Fig. 3-6, M&B28767-induced neurite retraction was completely inhibited in a cell microinjected with C3 exoenzyme, whereas M&B28767-induced morphological change was not inhibited in a cell microinjected with the buffer alone (data not shown), indicating that microinjection itself did not inhibit neurite retraction. These results demonstrate that the EP3 receptor-mediated neurite retraction is required for the activation of Rho.

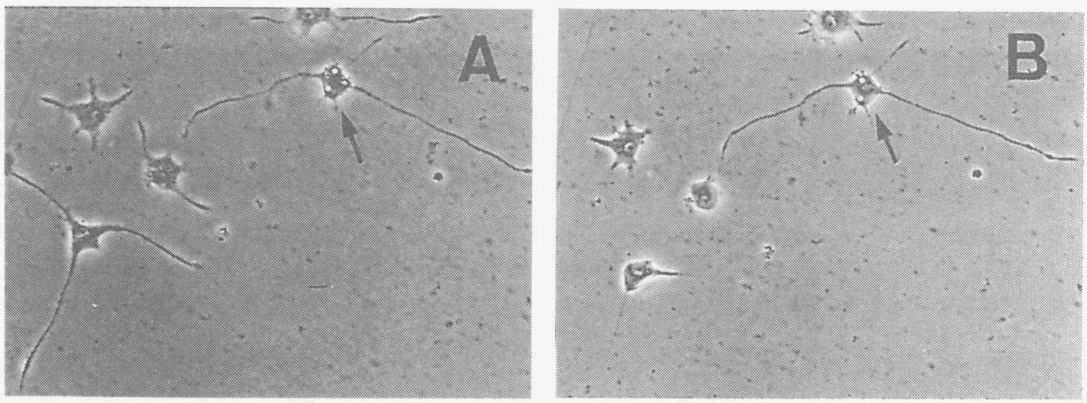

Figure 3-6. Effect of C3 exoenzyme on M&B28767-induced neurite retraction. Differentiated cells were microinjected with 100 μg/ml C3 (*A*) and then stimulated with 1 μM M&B28767 for 60 min (*B*). M&B28767 was added 30 min after injection. The arrows indicate injected cells. The results shown are representative of three independent experiments. At least 20 cells were microinjected in each experiment for C3 exoenzyme and the control buffer, and all cells microinjected gave the described response. Bar represents 50 μm.

Effect of Depletion of Intracellular PKC on M&B28767-induced Neurite Retraction

As shown in Chapter 2, constitutively active $G\alpha_q$ induces Rho-dependent neurite retraction and cell rounding, and these morphological changes are required for activation of PKC. Therefore, I examined whether the morphological action of the EP3 receptor was mediated by the activation of PKC. Even though the cells had been exposed to 1 μM TPA during differentiation and endogenous PKC had been down-regulated, PC12 cells were normally differentiated by NGF and neurite

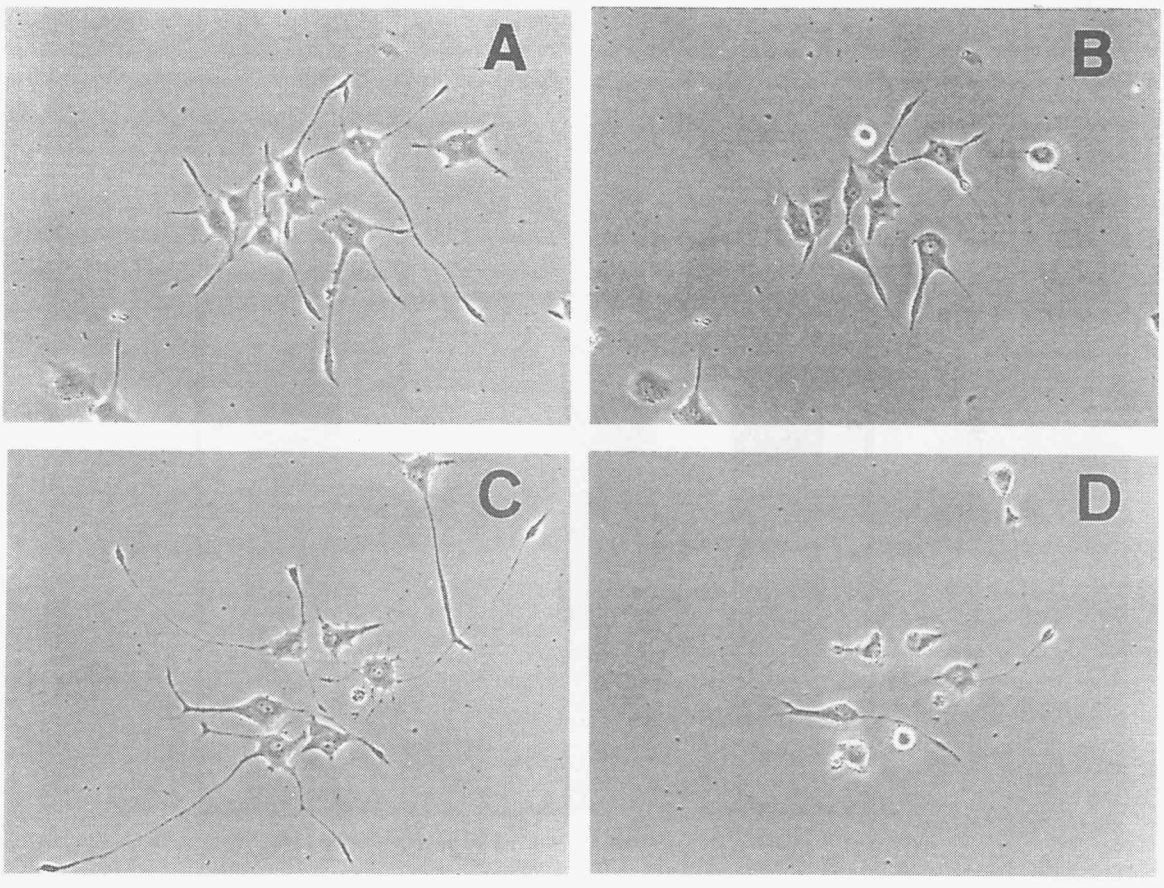

Figure 3-7. Effect of depletion of intracellular PKC on M&B28767-induced neurite retraction. (*A*) Cells were differentiated with NGF for 5 d. (*B*) Cells in *A* were exposed to 1 μM M&B28767 for 60 min. (*C*) Cells were differentiated with NGF for 5 d in the presence of 1 μM TPA. (*D*) Cells in *C* were exposed to 1 μM M&B28767 for 60 min. The results shown are representative of three independent experiments that yielded similar results. Bar represents 50 μm.

retraction induced by M&B28767 was not affected (Fig. 3-7 and 3-8). These results indicate that EP3 receptor-mediated morphological change does not involve the activation of PKC.

Effect of Tyrphostin A25 on M&B28767- or RhoA-Induced Neurite Retraction

As shown in Chapter 2, constitutively active $G\alpha_{13}$-induced neurite retraction was inhibited by a tyrosine kinase inhibitor tyrphostin A25. Therefore, I next examined whether tyrphostin A25 blocked M&B28767-induced neurite retraction in the NGF-differentiated PC12 cells. In the vehicle-treated cells, they retracted their extended neurites

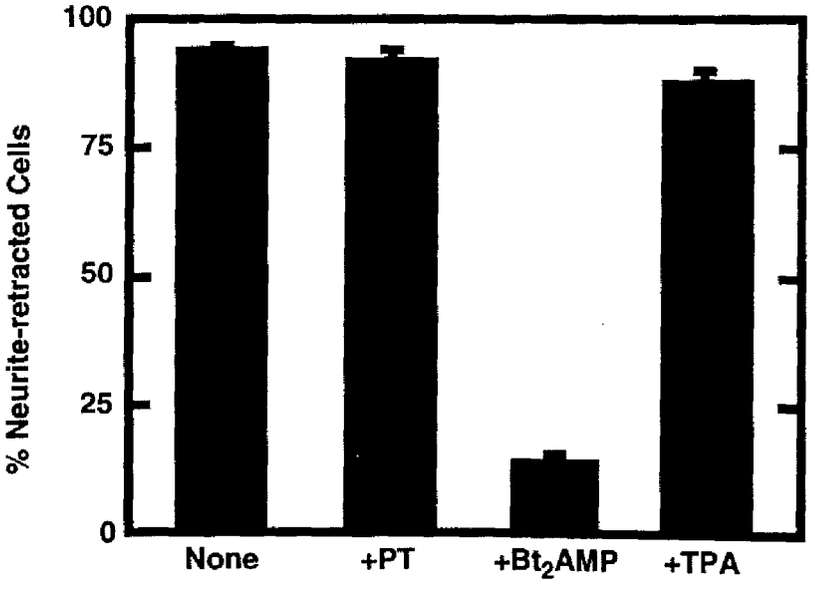

Figure 3-8. Quantification of effects of various reagents on M&B28767-induced neurite retraction. The percentages of neurite-retracted cells was determined as described under "Experimental Procedures". Data are means ± S.E. of triplicate experiments.

in response to 1 μM M&B28767 within 30 min (Fig. 3-9, *A* and *B*). In contrast, pretreatment of the cells with 300 μM tyrphostin A25 for 15 min blocked M&B28767-induced neurite retraction (Fig. 3-9, *C* and *D*). Fig. 3-11 shows the quantitative examination of the effect of tyrphostin A25. It decreased the percentage of the neurite-retracted cells in response to M&B28767 from 97.0 to 13.7%. The cells treated with tyrphostin A25 alone caused no morphological change for at least 60 min (data not shown). These results indicate that a tyrphostin A25-

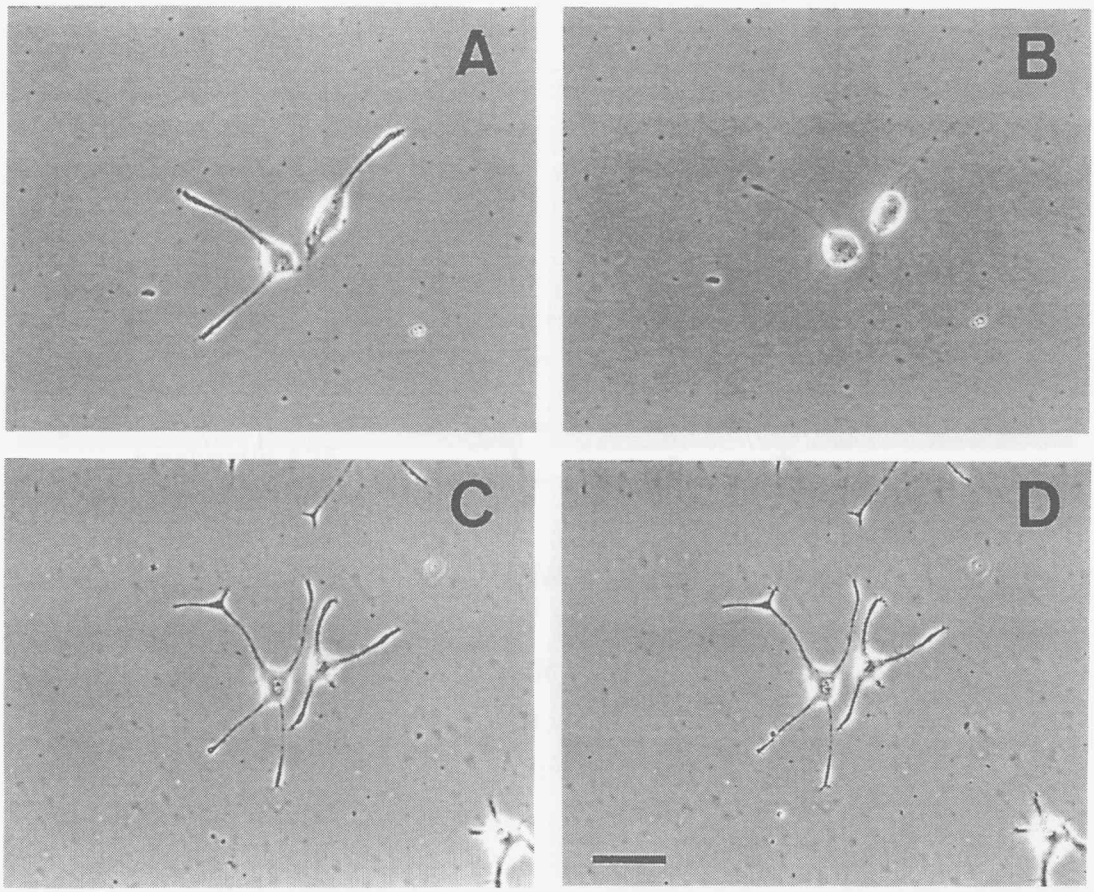

Figure 3-9. Effect of tyrphostin A25 on neurite retraction induced by M&B28767. The cells differentiated with NGF for 3 days were pretreated with vehicle (*A* and *B*) or 300 μM tyrphostin A25 (*C* and *D*) for 15 min. Then the cells were photographed before (*A* and *C*) and 30 min after (*B* and *D*) the addition of 1 μM M&B28767. The results shown are representative of three independent experiments. The *bar* represents 50 μm.

sensitive tyrosine kinase was involved in the EP3 receptor-mediated neurite retraction.

To determine whether this tyrphostin A25-sensitive tyrosine kinase functioned upstream or downstream of Rho, I next microinjected constitutively active RhoA, $RhoA^{V14}$, into the cytoplasm of the differentiated PC12 cells. More than 70% of the cells microinjected with 2 mg/ml of $RhoA^{V14}$ caused neurite retraction and cell rounding within 30 min. However, pretreatment of the cells with 300 μM

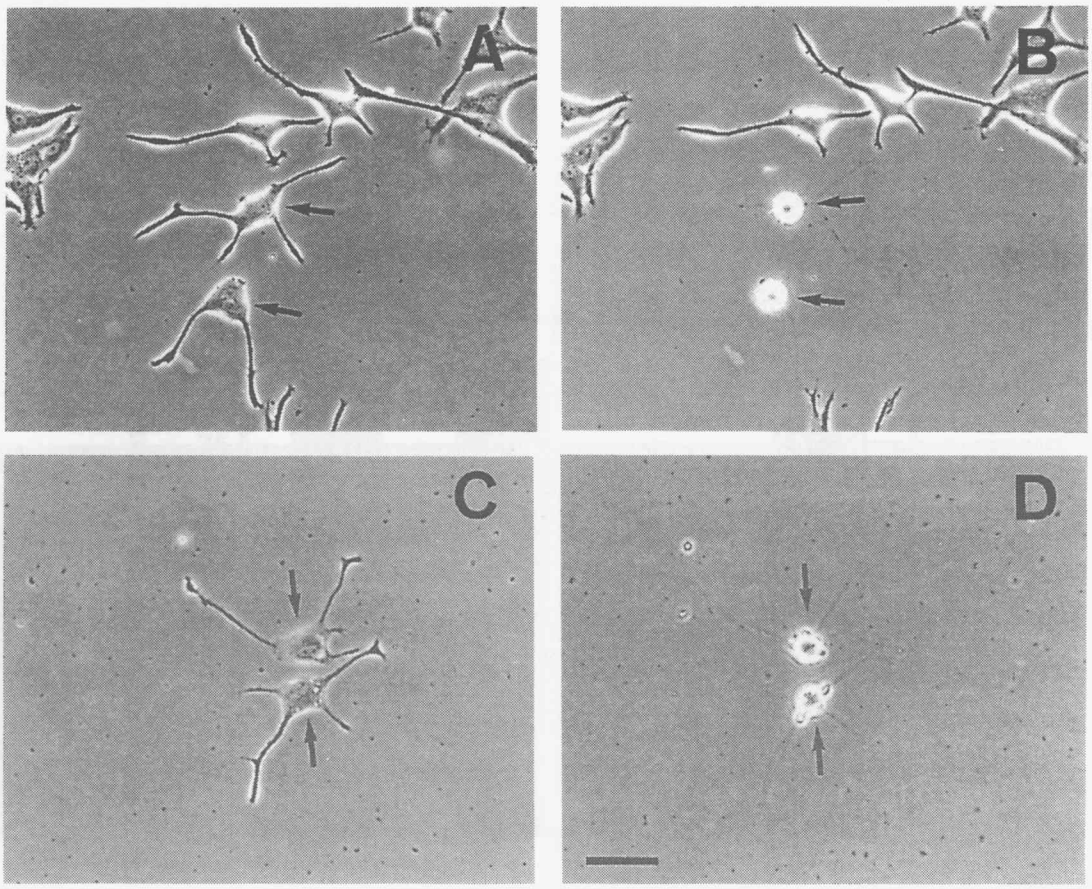

Figure 3-10. Effect of tyrphostin A25 on neurite retraction induced by $RhoA^{V14}$. The cells differentiated with NGF for 3 days were pretreated with vehicle (*A* and *B*) or 300 μM tyrphostin A25 (*C* and *D*) for 15 min. Then the cells were photographed before (*A* and *C*) and 30 min after (*B* and *D*) microinjection of 2 mg/ml $RhoA^{V14}$. The *arrows* indicate injected cells. The results shown are representative of three independent experiments. The *bar* represents 50 μm.

tyrphostin A25 for 15 min did not blocked neurite retraction induced by microinjection of RhoA^{V14} (Fig. 3-10, and Fig. 3-11). These results indicate that a tyrphostin A25-sensitive tyrosine kinase is not involved in the neurite retraction induced by Rho.

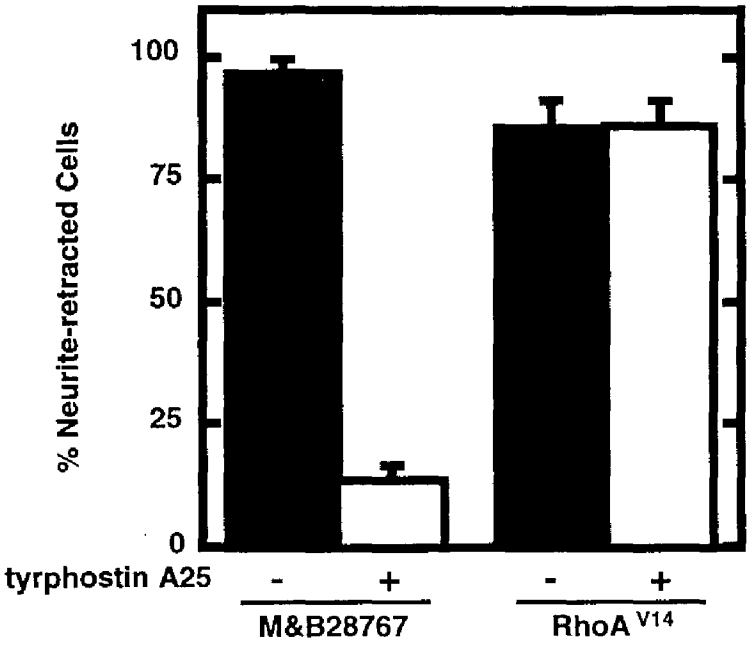

Figure 3-11. Quantification of effect of tyrphostin A25 on neurite retraction induced by M&B28767 and RhoA^{V14}. The cells differentiated with NGF for 3 days were pretreated with vehicle (-Tyr) or 300 μM tyrphostin A25 (+Tyr) for 15 min. Then the cells were exposed to 1 μM M&B28767 or microinjected with 2 mg/ml RhoA^{V14}. The percentages of neurite-retracted cells were determined 30 min after the addition of the agonist or microinjection of RhoA^{V14}, as described under "Experimental Procedures". Data are the mean ± S.E. of triplicate experiments.

Discussion

Information on the function of EP3 receptors in the nervous system is scarce, although several findings have been reported, for example, they inhibit neurotransmitter release and have hyperalgesic effects (92, 93). In this study, I described a new possible function of EP3 receptors, modulation of a neuronal morphological change through a novel pathway distinct from adenylate cyclase inhibition or PKC activation. In EP3 receptor-expressing PC12 cells differentiated with NGF, M&B28767 induced neurite retraction. However, no morphological change was caused by the agonist in untransfected cells, indicating that M&B28767-induced neurite retraction is mediated by EP3 receptor.

Growing evidence suggests that Rho plays a key role in the regulation of the actin cytoskeleton. The functions of Rho have been explored using the C3 exoenzyme, which ADP-ribosylates and inactivates Rho protein (15, 16). Many studies using C3 exoenzyme demonstrated that Rho is involved in the control of cell shape, adhesion, and motility by regulating the actin cytoskeleton in fibroblasts (3), and it is also involved in neurite retraction in neuronal cells (17). Since microinjection into the EP3 receptor-expressing cells with the C3 exoenzyme completely inhibited M&B28767-induced neurite retraction (Fig. 3-6), Rho was shown to be an essential element in the EP3 receptor-mediated neurite retraction.

Among classical second messenger pathways, EP3 receptor is coupled to adenylate cyclase inhibition through Gi in PC12 cells, but the receptor stimulates neither adenylate cyclase nor PLC, indicating that EP3 receptor is exclusively coupled to Gi. However, neurite retraction mediated by this receptor was not suppressed by PT treatment (Figs. 3-4

and 3-8), indicating that G_i is not involved in the EP3 receptor-mediated neurite retraction. In Chapter 2, expression of constitutively active mutants of $G\alpha_{12}$, $G\alpha_{13}$, and $G\alpha_q$ induced Rho-dependent neurite retraction and cell rounding in NGF-differentiated PC12 cells. Among these $G\alpha$ subunits, $G\alpha_{13}$- and $G\alpha_q$-induced neuronal morphological changes were blocked by tyrphostin A25, whereas the morphological changes by $G\alpha_{12}$ were not influenced by this tyrosine kinase inhibitor. Because tyrphostin A25 blocked the EP3 receptor-mediated neurite retraction, $G\alpha_{12}$ does not appear to mediate the signaling from EP3 receptor to Rho activation. Neuronal morphological changes by $G\alpha_q$ also required activation of PKC and Ca^{2+} influx. However, activation of the EP3 receptor did not increase intracellular Ca^{2+} concentration in the PC12 cells, and the neuronal morphological changes by the EP3 receptor were not blocked by inhibition of PKC activity (Figs. 2-7 and 2-8) or elimination of extracellular Ca^{2+} (data not shown). Taken together, these results suggest that $G\alpha_{13}$ may be involved in the EP3 receptor-mediated Rho activation leading to neurite retraction in the differentiated PC12 cells.

I examined the regulation of the EP3 receptor-mediated neurite retraction by PKA, and revealed that activation of PKA inhibited EP3 receptor-mediated neurite retraction, indicating that PKA is a negative regulator. As the potential PKA phosphorylation site is located in the first cytoplasmic loop of the EP3 receptor, it is possible that PKA phosphorylates the EP3 receptor. The phosphorylation of this site by PKA may stop the EP3 receptor-mediated signaling. The second possible site of the action of PKA is on a downstream component. LPA-induced neurite retraction was recently reported to be prevented by pretreatment with Bt_2cAMP in PC12 cells (37). Furthermore, it was recently reported that PKA directly phosphorylated Rho and this

phosphorylation resulted in termination of Rho signaling (94). As LPA and EP3 receptors use different pathways to activate Rho, PKA may block Rho-mediated morphological regulation by phosphorylating Rho in PC12 cells.

From this study, we propose new possible functions of PGE_2 acting through EP3 receptors in the nervous system. EP3 receptors have been shown to be expressed in a variety of neurons in the brain (90, 91), and neurons in the dorsal root ganglion (95). PGE_2 is normally produced in the brain, and its production is dramatically stimulated by brain injuries, such as concussion, trauma, and asphyxia (96-99). When the brain is injured, newly synthesized PGE_2 may retract the neurites of EP3 receptor-expressing neurons and reorganize damaged neuronal connections. In addition, the levels of PGE_2 are also increased in the brain by synaptic activity or during development (100). Furthermore, cyclooxygenase, a rate-limiting enzyme in PG synthesis, has been reported to be markedly induced by seizures or N-methyl-D-aspartate-dependent synaptic activity, especially in the cortex and hippocampus (101), in which EP3 receptors are highly expressed (90). PGE_2 may be involved in refining and remodeling the initial neuronal connections through EP3 receptors.

In the present study, I have shown that EP3 receptor elicits neurite retraction in a Rho-dependent fashion. This study will contribute not only to the understanding of neuronal PGE_2 function, but it will also help to elucidate the molecular mechanisms of signal transduction pathways between heterotrimeric G protein-coupled receptors and Rho.

CONCLUSION

The summaries of the results obtained here are as follows:

1) p160 RhoA-binding kinase ROKα, a target for RhoA acts downstream of Rho to induce neurite retraction in PC12 cells.
2) Activation of $G\alpha_{12}$, $G\alpha_{13}$, and $G\alpha_q$ induces Rho-dependent neurite retraction in PC12 cells through different signaling pathways.
3) Prostaglandin EP3 receptor is coupled to $G\alpha_{13}$ causing neurite retraction through a Rho/Rho-associated kinase-dependent pathway in PC12 cells.

The present study will not only contribute to the understanding of the signal transduction pathway involving Rho in neuronal cells, but will also help to elucidate the molecular mechanisms for neuritogenesis and axonal pathfinding during neuronal development.

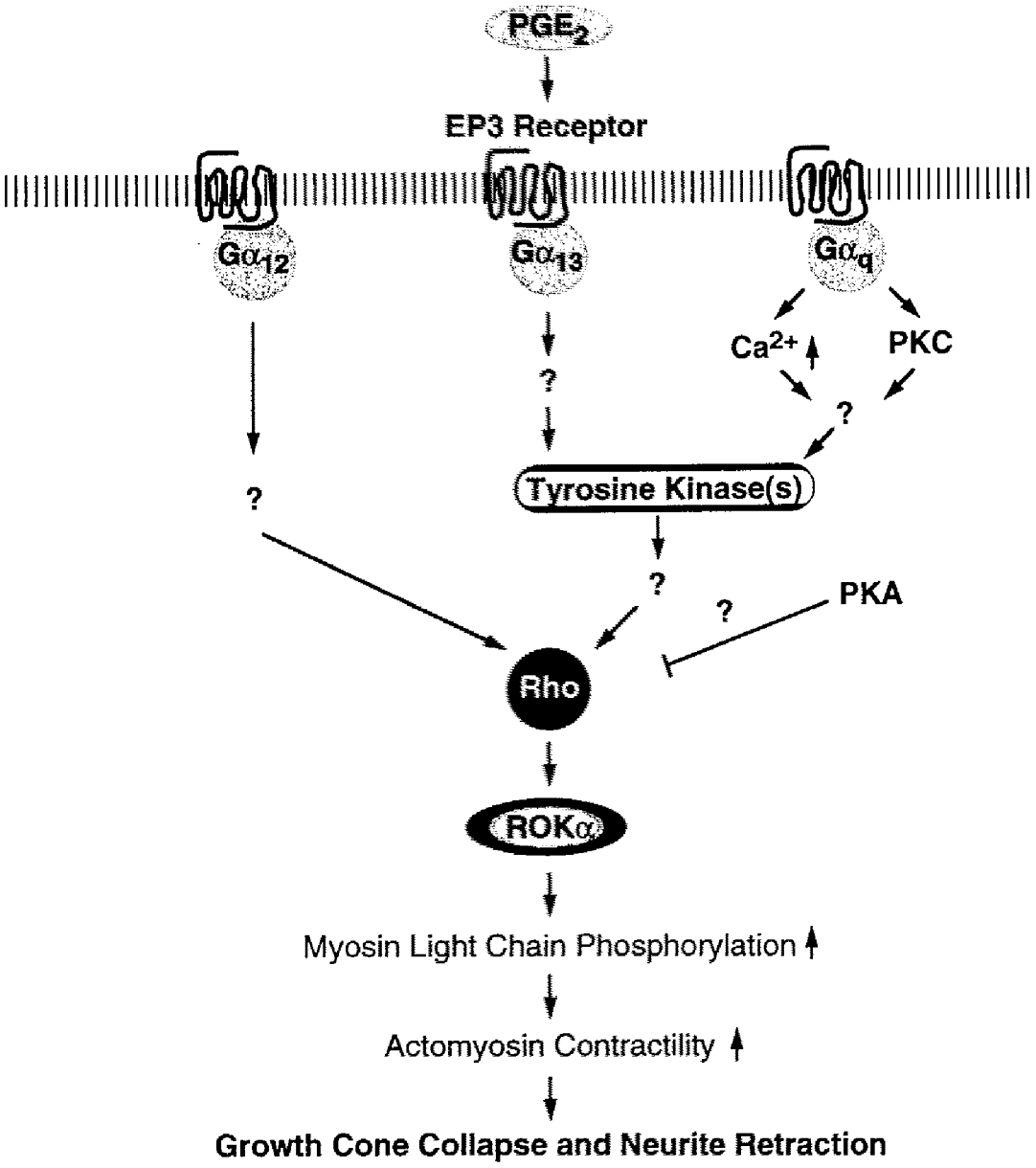
PGE2
EP3 Receptor
Gα12
Gα13
Gαq
Ca2+
PKC
?
?
?
Tyrosine Kinase(s)
?
?
PKA
Rho
ROKα
Myosin Light Chain Phosphorylation
Actomyosin Contractility
Growth Cone Collapse and Neurite Retraction

EXPERIMENTAL PROCEDURES

Materials

M&B28767 was a generous gift from Dr. M. P. L. Caton of Rhone-Poulene Ltd. NGF 2.5S was purchased from Promega Corporation, and *Clostridium botulinum* C3 exoenzyme was from Seikagaku Kogyo. Texas red-coupled dextran was from Molecular Probes, tyrphostin A25 and tyrphostin AG1478 were from Calbiochem, Ro31-8220 was from Nacalai Tesque, Bt_2cAMP was from Sigma, and TPA was from Funakoshi Pharmaceuticals. The sources of the other materials are shown in the text.

Expression and Purification of Recombinant Proteins

The coding region of human RhoA was generated by reverse transcription-PCR from HeLa cells using primers 5'-CTGGACTCGAA TTCGTTGCCTGAGCAATGG-3' and 5'-GCAAGATGAATTCTGATT TGTAATCTTAGG-3'. The PCR product was digested with EcoRI , cloned into the pBluescript KS(+), and completely sequenced. cDNAs for $RhoA^{V14}$ and $RhoA^{V14A37}$ were generated by PCR-mediated mutageneis (102), subcloned into the BamHI/EcoRI sites of pGEX-4T-2 vector, and sequenced. Recombinant $RhoA^{V14}$ and $RhoA^{V14A37}$ were expressed as GST fusion proteins in *E.coli*, and purified on glutathione-Sepharose beads according to the method of Self, A. J. and Hall, A. (103). The sequence encoding ROKα containing the catalytic domain (CD-ROKα, amino acids 1-543), the Rho-binding domain (RBD-ROKα, amino acids 932-1065), and the PH domain (PHD-ROKα, amino acids 1116-1379) were generated by reverse transcription-PCR from PC12 cells, using primers 5'-ATGAGCGGATCCCCGCCGACGGGGAAA-3' and 5'-ACCTTCTGAATTCATATCTGAGAGCTCTGG-3' for CD-

ROKα, 5'-GACGGATCCAAAGAGAAGATCATGAAAGAGC-3' and 5'-GTTGTGTGAATTCTTAACGTTCAG-3' for RBD-ROKα, and 5'-TCGCAGGGATCCGCCTTGCATATTGG-3' and 5'-TCTTGTGGATG GAAGAATTCGATCACCTTC-3' for PHD-ROKα, respectively. The kinase-deficient mutant of CD-ROKα (CD-ROKα^{K112G}) was generated by PCR-mediated mutageneis. All PCR products for each domain of ROKα were cloned into the pCR2.1 vector and sequenced completely. The PCR products for RBD-ROKα and PHD-ROKα were subcloned into the BamHI/EcoRI sites of pGEX-4T-2 vector, and recombinant proteins were expressed as GST fusion proteins in *E.coli* and purified on glutathione-Sepharose beads. The PCR products for CD-ROKα and CD-ROKα^{K112G} were subcloned into the BamHI/EcoRI sites of pAcG2T vector, and recombinant proteins were expressed as GST fusion proteins in Sf9 cells with BaculoGold™ system (PharMingen) and purified on glutathione-Sepharose beads according to the method of Matsui, T. et al. (23). All recombinant proteins were dialyzed with an injection buffer (10 mM Tris-HCl, pH 7.6, 150 mM NaCl, 2 mM $MgCl_2$, and 0.1 mM dithiothreitol) at 4 °C overnight for microinjection. Protein concentration was determined by comparing with bovine serum albumin standards after electrophoresis on a SDS-polyacrylamide gel and staining with Coomassie Brilliant Blue. Purified proteins showed only one band on Coomassie-stained gel.

Construction of Mammalian Expression Plasmids

Wild type mouse $G\alpha_{12}$ and $G\alpha_{13}$ were generous gifts from Dr. M. I. Simon (California Institute of Technology). Wild type rat $G\alpha_{i2}$ was kindly provided from Dr. T. Katada (Tokyo University). Mammalian expression vector pEF-BOS was kindly provided from Dr. S. Nagata (Osaka University). Wild type mouse $G\alpha_q$ was generated by reverse

transcription-PCR from mouse brain using primers 5'-GAGGCACTTC GGAAGAATGA-3' and 5'-AAGAACCAGTTTCTGGGAGG-3', and the PCR product was cloned into the pCR2.1 vector and sequenced completely. The cDNAs of the constitutively active mutants of $G\alpha_{12}$ ($G\alpha_{12}$Q229L; $G\alpha_{12}$QL), $G\alpha_{13}$ ($G\alpha_{13}$Q226L; $G\alpha_{13}$QL), $G\alpha_q$ ($G\alpha_q$Q209L; $G\alpha_q$QL), $G\alpha_{i2}$ ($G\alpha_{i2}$Q205L; $G\alpha_{i2}$QL), and the cDNA of $RhoA^{N19}$ were generated by PCR-mediated mutagenesis (102), and sequenced completely. The cDNAs of constitutively active mutants of $G\alpha$ subunits were inserted into the pcDNA3 expression vector (Invitrogen), and the cDNAs of $RhoA^{V14}$ and $RhoA^{N19}$ were inserted into pEF-BOS.

Cell Culture and Microinjection

PC12 cells were cultured in Dulbecco's modified Eagle's medium (DMEM) containing 5% fetal bovine serum, 10% horse serum, 4 mM glutamine, 100 units/ml penicillin, and 0.2 mg/ml streptomycin under humidified conditions in 95% air and 5% CO_2 at 37 °C. To obtain EP3 receptor-expressing PC12 cells, cDNA encoding the EP3B receptor was inserted into the expression vector, pcDNA3, and the plasmid constructed was transfected into PC12 cells by lipofection (104). Stable transformants were cloned by selection with 500 μg/ml of G418 (Gibco laboratories life technologies, Inc.). For microinjection, cells were seeded at a density 2 x 10^4 onto poly-D-lysine (Sigma)-coated 35 mm dishes, which were marked with a cross to facilitate the localization of injected cells. Microinjection was performed using an IMM-188 microinjection apparatus (Narishige). After cells had been differentiated in serum-free DMEM containing 50 ng/ml NGF for 3 or 4 days, 30 μg/ml of the indicated plasmids were microinjected into the nucleus with 1 mg/ml Texas red-coupled dextran to visualize injected

cells, or 2 mg/ml of recombinant proteins were microinjected into the cytoplasm. During microinjection, differentiated cells were maintained in Hepes-buffered DMEM (pH 7.4) at 37 °C. After microinjection, cells were replaced into NGF-containing serum-free DMEM and incubated for the indicated times. To examine the effect of extracellular Ca^{2+}, microinjected cells were replaced into Hepes-buffered saline containing 140 mM NaCl, 4.7 mM KCl, 5 mM $MgCl_2$, 1.2 mM KH_2PO_4, 11 mM glucose, 2 mM EGTA, and 15 mM Hepes, pH 7.4. Cells were photographed at x 400 magnification under the microscope with phase contrast or by fluorescence of Texas red-coupled dextran. A neurite was identified as a process greater than one cell body diameter in length. For the quantitative examinations in Chapters 1 and 3, neurite-retracted cells were defined as the cells that retracted by more than 10% of their original length within 30 min of the addition of the agonist or of the microinjection of recombinant proteins. For the quantitative examinations in Chapter 2, neurite-retracted cells were defined as the cells that almost completely retracted their neurites and caused rounding of the cell body within 3 h of the microinjection of plasmids. To establish the time course in Chapter 3, the average neurite length was measured from at least 30 cells in the same field, excluding the cells that did not respond to the agonist. The percentages of neurite-retracted cells were calculated by counting at least 30 microinjected cells in the same field, and all data were obtained from triplicate experiments.

MLC Phosphorylation Assay

MLC phosphorylation assay was performed according to the method of Amano et al. (28). The kinase reaction for ROKα was carried out in 50 μl of the reaction mixture (50 mM Tris-HCl (pH 7.5), 2 mM EDTA, 1mM dithiothreitol, 7 mM $MgCl_2$, 0.1% 3-[(3-

cholamidopropyl)dimethylammonio]-1-propanesulfonic acid, 250 μM [γ-^{32}P]ATP (2.5 GBq/mmol), and 4 μg of purified MLC) with each GST fusion protein (10 ng). After an incubation for 10 min at 30 °C, the reaction mixtures were boiled in SDS-sample buffer and subjected to SDS-PAGE. The radiolabeled bands were visualized by an image analyzer (Fuji).

ACKNOWLEDGMENTS

The auther appreciates gratefully to Professor Manabu Negishi, Graduate School of Biostudies, Kyoto University, for his kind and constant guidance through the course of this work.

The auther's appreciation is also given to Professor Atsushi Ichikawa, Graduate School of Pharmaceutical Sciences, Kyoto University, for his continuous support.

And the auther as well thanks members of the Laboratory of Molecular Neurobiology, Graduate School of Biostudies, Kyoto University, for their helpful discussions and technical supports.

Last, the auther heartily thanks my wife Yukiko and my parents for their mental encouragement and persistent understanding and here dedicate this thesis to them.

PUBLICATIONS LIST

Chapter 1

Hironori Katoh, Junko Aoki, Atsushi Ichikawa, and Manabu Negishi (1998) p160 RhoA-Binding Kinase ROKα Induces Neurite Retraction. *J. Biol. Chem.* **273,** 2489-2492.

Chapter 2

Hironori Katoh, Junko Aoki, Yoshiaki Yamaguchi, Yoshimi Kitano, Atsushi Ichikawa, and Manabu Negishi (1998) Constitutively Active $G\alpha_{12}$, $G\alpha_{13}$, and $G\alpha_q$ Induce Rho-dependent Neurite Retraction through Different Signaling Pathways. *J. Biol. Chem.* **273,** 28700-28707.

Chapter 3

Hironori Katoh, Manabu Negishi, and Atsushi Ichikawa (1996) Prostaglandin E Receptor EP3 Subtype Induces Neurite Retraction via Small GTPase Rho. *J. Biol. Chem.* **271,** 29780-29784.

Junko Aoki, Hironori Katoh, Hidekazu Yasui, Yoshiaki Yamaguchi, Kazuhiro Nakamura, Hiroshi Hasegawa, Atsushi Ichikawa and Manabu Negishi (1999) Signal Transduction Pathway Regulating Prostaglandin EP3 Receptor-induced Neurite Retraction. *Biochem. J.* **340,** 365-369.

REFERENCES

1. Goodman, C. S., and Shatz, C. J. (1993) *Cell* **10** (Suppl.), 77-98.
2. Keynes, R., and Cook, G. M. W. (1995) *Cell* **83,** 161-169.
3. Hall, A. (1998) *Science* **279,** 509-514.
4. Kaibuchi, K., Kuroda, S., and Amano, M. (1999) *Annu. Rev. Biochem.* **68,** 459-486.
5. Kozma, R., Sarner, S., Ahmed, S., and Lim, L. (1997) *Mol. Cell. Biol.* **17,** 1201-1211.
6. Gebbink, M. F. B. G., Kranenburg, O., Poland, M., Horck, F. P. G., Houssa, B., and Moolenaar, W. H. (1997) *J. Cell Biol.* **137,** 1603-1613.
7. Daniels, R. H., Hall P. S., and Bokoch, G. M. (1998) *EMBO J.* **17,** 754-764.
8. Luo, L., Jan, L. Y., and Jan, Y.-N. (1997) *Curr. Opin. Neurobiol.* **7,** 81-86.
9. Threadgill, R., Bobb, K., and Ghosh, A. (1997) *Neuron* **19,** 625-634.
10. Ruchhoeft, M. L., Ohnuma, S., McNeill, L., Holt, C. E., and Harris, W. A. (1999) *J. Neurosci.* **19,** 8454-8463.
11. Greene, L. A., and Tischler, A. S. (1976) *Proc. Natl. Acad. Sci. U. S. A.* **73,** 2424-2428.
12. Tigyi, G., and Miledi, R. (1992) *J. Biol. Chem.* **267,** 21360-21367.
13. Dyer, D., Tigyi, G., and Miledi, R. (1992) *Mol. Brain Res.* **14,** 293-301.
14. Sato, K., Tomura, H., Igarashi, Y., Ui, M., and Okajima, F. (1997) *Biochem. Biophys. Res. Commun.* **240,** 329-334.
15. Aktories, K., Weller, U., and Chhatwal, G. S. (1987) *FEBS Lett.* **212,** 109-113.
16. Sekine, A., Fujiwara, M., and Narumiya, S. (1989) *J. Biol. Chem.* **264,** 8602-8605.
17. Jalink, K., Corven, E. J., Hengeveld, T., Morii, N., Narumiya, S., and Moolenaar, W. H. (1994) *J. Cell Biol.* **126,** 801-810.

18. Tigyi, G., Fischer, D. J., Sebök, Á., Yang, C., Dyer, D. L., and Miledi, R. (1996) *J. Neurochem.* **66,** 537-548.

19. Watanabe, G., Saito, Y., Madaule, P., Ishizaki, T., Fujisawa, K., Morii, N., Mukai, H., Ono, Y., Kakizuka, A., and Narumiya, S. (1996) *Science* **271,** 645-648.

20. Amano, M., Mukai, H., Ono, Y., Chihara, K., Matsui, T., Hamajima, Y., Okawa, K., Iwamatsu, A., and Kaibuchi, K. (1996) *Science* **271,** 648-650.

21. Leung, T., Manser, E., Tan, L., and Lim, L. (1995) *J. Biol. Chem.* **270,** 29051-29054.

22. Matsui, T., Amano, M., Yamamoto, T., Chihara, K., Nakafuku, M., Ito, M., Nakano, T., Okawa, K., Iwamatsu, A., and Kaibuchi, K. (1996) *EMBO J.* **15,** 2208-2216.

23. Nakagawa, O., Fujisawa, K., Ishizaki, T., Saito, Y., Nakao, K., and Narumiya, S. (1996) *FEBS lett.* **392,** 189-193.

24. Reid, T., Furuyashiki, T., Ishizaki, T., Watanabe, G., Watanabe, N., Fujisawa, K., Morii, N., Madaule, P., and Narumiya, S. (1996) *J. Biol. Chem.* **271,** 13556-13560.

25. Watanabe, N., Madaule, P., Reid, T., Ishizaki, T., Watanabe, G., Kakizuka, A., Saito, Y., Nakao, K., Jockusch, B., M., and Narumiya, S. (1997) *EMBO J.* **16,** 3044-3056.

26. Kimura, K., Ito, M., Amano, M., Chihara, K., Fukuta, Y., Nakafuku, M., Yamamori, B., Feng, J., Nakano, T., Okawa, K., Iwamatsu, A., and Kaibuchi, K. (1996) *Science* **273,** 245-248.

27. Amano, M., Ito, M., Kimura, K., Fukuta, Y., Chihara, K., Nakano, T., Matsuura, Y., and Kaibuchi, K. (1996) *J. Biol. Chem.* **271,** 20246-20249

28. Leung, T., Chen, X.-Q., Manser, E., and Lim, L. (1996) *Mol. Cell. Biol.* **16,** 5313-5327.

29. Amano, M., Chihara, K., Kimura, K., Fukuta, Y., Nakamura, N., Matsuura, Y., and Kaibuchi, K. (1997) *Science* **275,** 1308-1311.

30. Yasui, Y., Amano, M., Nagata, K., Inagaki, N., Nakamura, H., Saya, H., Kaibuchi, K., and Inagaki, M. (1998) *J. Cell Biol.* **143,** 1249-1258.

31. Katoh, H., Negishi, M., and Ichikawa, A. (1996) *J. Biol. Chem.* **271,** 29780-29784.

32. Jalink, K., Eichholtz, T., Postma, F. R., Coven, E. J., and Moolenaar, W. H. (1993) *Cell Growth Differ.* **4,** 247-255.

33. Kosako, H., Amano, M., Yanagida, M., Tanebe, K., Nishi, Y., Kaibuchi, K., and Inagaki, M. (1997) *J. Biol. Chem.* **272,** 10333-10336.

34. Hashimoto, R., Nakamura, Y., Kosako, H., Amano, M., Kaibuchi, K., Inagaki, M., and Takeda, M. (1999) *Biochem. Biophys. Res. Commun.* **263,** 575-579.

35. Postma, F. R., Jalink, K., Hengeveld, T., and Moolenaar, W. H. (1996) *EMBO J.* **15,** 2388-2395.

36. Jalink, K., and Moolenaar, W. H. (1992) *J. Cell Biol.* **118**, 411-419.

37. Tigyi, G., Fischer, D. J., Sebök, À., Yang, C., Dyer, D. L., and Miledi, R. (1996) *J. Neurochem.* **66,** 549-558.

38. Strathmann M. P., and Simon, M. I. (1991) *Proc. Natl. Acad. Sci. U. S. A.* **88,** 5582-5586.

39. Xu, N., Bradley, L., Ambudukar, I., and Gutkind, J. S. (1993) *Proc. Natl. Acad. Sci. U. S. A.* **90,** 6741-6745.

40. Voyno-Yasenetskya, T. A., Pace, A. M., and Bourne, H. R. (1994) *Oncogene* **9,** 2559-2565.

41. Prasad, M. V. V. S. V., Dermott, J. M., Heasley, L. E., Johnson, G. L., and Dhanasekaran, N. (1995) *J. Biol. Chem.* **270,** 18655-18659.

42. Collins, L. R., Minden, A., Karin, M., and Brown, J. H. (1996) *J. Biol. Chem.* **271,** 17349-17353.

43. Voyno-Yasenetskya, T. A., Faure, M. P., Ahn, N. G., and Bourne, H. R. (1996) *J. Biol. Chem.* **271,** 21081-21087.

44. Buhl, A. M., Johnson, N. L., Dhanasekaran, N., and Johnson, G. L. (1995) *J. Biol. Chem.* **270,** 24631-24634.

45. Gohla, A., Harhammer, R., and Schultz, G. (1998) *J. Biol. Chem.* **273,** 4653-4659.

46. Voyno-Yasenetskya, T. A., Conklin, B. R., Gilbert, R. L., Hooiyey, R., Bourne, H. R., and Barber, D. L. (1994) *J. Biol. Chem.* **269,** 4721-4724.

47. Hooley, R., Chunn-Yuan, T., Symons, M., and Barber, D. L. (1996) *J. Biol. Chem.* **271,** 6152-6158.

48. Lin, X., Voyno-Yasenetskya, T. A., Hooley, R., Lin. C.-Y., Orlowski, J., and Barber, D. L. (1996) *J. Biol. Chem.* **271,** 22604-22610.

49. Plonk, S. G., Park, S.-K., and Exton, J. H. (1998) *J. Biol. Chem.* **273,** 4823-4826.

50. Althoefer, H., Eversole-Cire, P., and Simon, M. I. (1997) *J. Biol. Chem.* **272,** 24380-24386.

51. Masters, S. B., Tyler Miller, R., Chi, M.-H., Chang, F.-H., Beiderman, B., Lopez, N. G., and Bourne, H. R. (1989) *J. Biol. Chem.* **264,** 15467-15474.

52. Osawa, S., Danasekaran, N., Woon, C. W., and Johnson, G. L. (1990) *Cell* **63,** 697-706.

53. Nobes, C. D., Hawkins, P., Stephens, L., and Hall. A. (1995) *J. Cell Sci.* **108,** 225-233.

54. Matthies, H. J. G., Palfrey, H. C., Hirning, L. D., and Miller, R. J. (1987) *J. Neurosci.* **7,** 1198-1206.

55. Danasekaran, N., and Dermott, J. M. (1996) *Cell. Signal.* **8,** 235-245.

56. Dhanasekaran, N., Vara Prasad, M. V. V. S., Wadsworth, S. J., Dermott, J. M., and van Rossum, G. (1994) *J. Biol. Chem.* **269,** 11802-11806.

57. Wadsworth, S. J., Gebauer, G., van Rossum, G., and Danasekaran, N. (1997) *J. Biol. Chem.* **272,** 28829-28832.

58. Kuno, M., and Gardner, P. (1987) *Nature* **326,** 301-304.

59. Irvine, R. F., and Moor, R. M. (1986) *Biochem. J.* **240,** 917-920.

60. Mochizuki-Oda, N., Nakajima, Y., Nakanishi, S., and Ito, S. (1994) *J. Biol. Chem.* **269,** 9651-9658.

61. Lev, S., Moreno, H., Martinez, R., Canoll, P., Peles, E., Musacchio, J. M., Plowman, G. D., Rudy, B., and Schlessinger, J. (1995) *Nature* **376,** 737-745.

62. Heasley, L. E., Storey, B., Fanger, G. R., Butterfield, L., Zamarripa, J., Blumberg, D., and Maue, R. A. (1996) *Mol. Cell. Biol.* **16,** 648-656.

63. Zheng, Y., Olson, M. F., Hall, A., Cerione, R. A., and Toksoz, D. (1995) *J. Biol. Chem.* **270,** 9031-9034.

64. Glaven, J. A., Whitehead, I. P., Nomanbhoy, T., Kay, R., and Cerione, R. A. (1996) *J. Biol. Chem.* **271,** 27374-27381.

65. Hart, M. J., Sharma, S., elMasry, N., Qiu, R.-G., McCabe, P., Polakis, P., and Bollag, G. (1996) *J. Biol. Chem.* **271,** 25452-25458.

66. Jin, Z., and Strittmatter, S. M. (1997) *J. Neurosci.* **17,** 6256-6263.

67. Threadgill, R., Bobb, K., and Ghosh, A. (1997) *Neuron* **19,** 625-634.

68. Wolfe, L. S. (1982) *J. Neurochem.* **38,** 1-14.

69. Milton,A. S., and Wendlandt, S. (1970) *J. Physiol., Lond.* **207,** 76-77.

70. Stitt, J. T. (1986) *Yale J. biol. Med.* **59,** 137-149.

71. Ojeda, S. R., and Campbel, W. B. (1982) *Endocrinology.* **111,** 1031-1037.

72. Ferreira, S. H. (1972) *Nature New Biol.* **240,** 200-203.

73. Roberts, P. J., and Hillier, K. (1976) *Brain Res.* **112,** 425-428.

74. Reimann, W., Steinhauser, H. B., Hedler, L., Starke, K., and Hertting, G. (1981) *Eur. J. Pharmacol.* **69,** 421-427.

75. Hölscher, C. (1995) *Eur. J. Pharm.* **294,** 253-259.

76. Negishi, M., Sugimoto, Y., and Ichikawa, A. (1995) *Biochim. Biophys. Acta.* **1259,** 109-120.

77. Coleman, R. A., Kennedy, I., Humphrey, P. P. A., Bunce, K., and Lumley, P. (1990) In *Comprehensive Medicinal Chemistry* (Hansch, C., Sammes, P. G., Taylor, J. B., and Emmett, J. C. eds.) **3,** 643-714 Pergamon Press, Oxford.

78. Coleman, R. A., Grix, S. P., Head, S. A., Louttit, J. B., Mallett, A., and Sheldrick, R. L. J. (1994) *Prostaglandins* **47,** 151-168.

79. Krall J. F., Barrett J. D., Jamgotchian N. J. and Korenman S. G. (1984) *J. Endocrinol.* **102,** 329-336.

80. Chen M. C. Y., Amirian D. A., Toomey M., Sanders M. J. and Soll A. H. (1988) *Gastroenterology* **94,** 1121-1129.

81. Ohia S. E. and Jumblatt J. E. (1990) *J. Pharmacol. Exp. Therap.* **255,** 11-16.

82. Richelsen B. and Beck-Nielsen N. (1984) *J. Lipid Res.* **26,** 127-134.

83. Garcia-Perez A. and Smith W. L. (1984) *J. Clin. Invest.* **74,** 63-74.

84. Negishi, M., Ito, S. and Hayaishi, O. (1989) *J. Biol. Chem.* **264,** 3916-3923.

85. Namba T., Sugimoto Y., Negishi M., Irie A., Ushikubi F., Kakizuka A., Ito S., Ichikawa A. and Narumiya S. (1993) *Nature* **365,** 166-170.

86. Watabe, A., Sugimoto, Y., Honda, A., Irie, A., Namba, T., Negishi, M., Narumiya, S., and Ichikawa, A. (1993) *J. Biol. Chem.* **268,** 20175-20178.

87. Katsuyama, M., Nishigaki, N., Sugimoto, Y., Morimoto, K., Negishi, M., Narumiya, S., and Ichikawa, A. (1995) *FEBS Lett.* **372,** 151-156.

88. Sugimoto, Y., Namba, T., Honda, A., Hayashi, Y., Negishi, M., Ichikawa, A, and Narumiya, S. (1992) *J. Biol. Chem.* **267,** 6463-6466.

89. Honda, A., Sugimoto, Y., Namba, T., Watabe, A., Irie, A., Negishi, M., Narumiya, S., and Ichikawa, A. (1993) *J. Biol. Chem.* **268,** 7759-7762.

90. Sugimoto, Y., Shigemoto, R., Namba, T., Negishi, M., Mizuno, N., Narumiya, S., and Ichikawa, A. (1994) *Neurosci.* **62,** 919-928.

91. Nakamura, K., Kaneko, T., Yamashita, Y., Hasegawa, H., Katoh, K., Ichikawa, A., and Negishi, M. (1999) *Neurosci. Lett.* **260,** 117-120.

92. Exner, H. J., and Schlicker, E. (1995) *Naunyn-Schmiedeberg's Arch. Pharmacol.* **351,** 46-52.

93. Kumazawa, T., Mizumura, K., and Koda, H. (1993) *Brain Res.* **632,** 321-324.

94. Lang, P., Gesbert, F., Carmagnat, M. D., Stancou, R., Pouchelet, M., and Bertoglio, J. (1996) *EMBO J.* **15,** 510-519.

95. Oida, H., Namba, T., Sugimoto, Y., Ushikubi, F., Ohishi, H., Ichikawa, A., and Narumiya, S. (1995) *Br. J. Phamacol.* **116,** 2828-2837.

96. Ment, L. R., Stewart, W. B., Duncan, C. C., Pitt, B. R., and Cole, J. (1987) *J. Neurosurg.* **67,** 278-283.

97. Shohami, E., Shapira, Y., Sidi, A., and Cotev, S. (1987) *J. Cereb. Blood Flow Metab.* **7,** 58-63.

98. Dewitt, D. S., Kong, D. L., Lyeth, B. G., Jenkins, L. W., Hayes, R. L., Wooten, E. D., and Prough, D. S. (1988) *J. Neurotrauma.* **5,** 303-313.

99. Ellis, E. F., Police, R. J., Rice, L. Y., Grabeel, M., and Holt, S. (1989) *J. Neurotrauma.* **6,** 31-37.

100. Hertting, G., and Seregi, A. (1989) In *The Arachidonic Acid Cascade in the Nervous System.* Part II, 84-99.

101. Yamagata, K., Andreasson, K. I., Kaufmann, W. E., Barnes, C. A., and Worley, P. F. (1993) *Neuron* **11,** 371-386.

102. Ito, W., Ishiguro, H., and Kurosawa, Y. (1991) *Gene* **102,** 67-70.

103. Self, A. J., and Hall, A. (1995) *Methods Enzymol.* **256,** 3-10.

104. Felgner, P. L., Gadek, T. R., Holm, M., Roman, R., Chan, H. W., Wenz, M., Northrop, J. P., Ringold, G. M., and Danielsen, M. (1987) *Proc. Natl. Acad. Sci. U. S. A.* **84,** 7413-7417.